International Geology Review

ISSN: (Print) (Online) Journal homepage: https://www.tandfonline.com/loi/tigr20

# Jurassic-Lower Cretaceous siliceous rocks and black shales from allochthonous complexes of the Koryak-Western Kamchatka orogenic belt, East Asia

Nadezhda I. Filatova, Elena Konstantinovskaya & Valentina Vishnevskaya

**To cite this article:** Nadezhda I. Filatova, Elena Konstantinovskaya & Valentina Vishnevskaya (2022) Jurassic-Lower Cretaceous siliceous rocks and black shales from allochthonous complexes of the Koryak-Western Kamchatka orogenic belt, East Asia, International Geology Review, 64:3, 311-330, DOI: 10.1080/00206814.2020.1848649

**To link to this article:** https://doi.org/10.1080/00206814.2020.1848649

INTERNATIONAL GEOLOGY REVIEW
2022, VOL. 64, NO. 3, 311–330
https://doi.org/10.1080/00206814.2020.1848649

Taylor & Francis
Taylor & Francis Group

ARTICLE

Check for updates

# Jurassic-Lower Cretaceous siliceous rocks and black shales from allochthonous complexes of the Koryak-Western Kamchatka orogenic belt, East Asia

Nadezhda I. Filatova[a], Elena Konstantinovskaya[b] and Valentina Vishnevskaya[a]

[a]Geological Institute, Russian Academy of Sciences, Moscow, Russia; [b]Earth and Atmospheric Sciences Department, University of Alberta, Edmonton, Canada

**ABSTRACT**

Composition, stratigraphic and structural position of Jurassic-Lower Cretaceous radiolarian-rich siliceous rocks and black shales are described within allochthonous lithotectonic complexes of the Koryak-Western Kamchatka orogenic belt of East Asia. Comparative lithological and stratigraphic analysis of sedimentary units exposed in imbricated tectonic slices over a distance of more than 1000 km helped to restore a continuous succession of siliceous rocks from Hettangian to Barremian. The Jurassic-Lower Cretaceous siliceous succession is composed of Hettangian and Aalenian-Barremian haematitic jaspers and Sinemurian-Toarcian radiolarian-bearing pyrite-bearing organic-rich black cherts and siliceous shales. Allochthonous Jurassic-Lower Cretaceous siliceous successions of the Koryak-Kamchatka orogenic belt likely accumulated in some open pelagic domains of the Paleo-Pacific within the Izanagi-Kula plate at different paleo-latitudes from high (southern boreal) to subequatorial (northern Tethys) paleo-latitudes. Depositional environments of Sinemurian-Toarcian organic-rich black shales were characterized by euxinic deep-water paleo-oceanic settings with poor water circulation. Accumulation of the Toarcian black shale succession corresponds in time to a global Toarcian oceanic anoxic event, while deposition of regionally occurring Sinemurian-Pliensbachian black shales was likely controlled by local factors. Hettangian, Middle Jurassic to Upper Jurassic-Barremian haematitic jaspers accumulated under aerobic conditions with well-circulated waters enriched with oxygen.

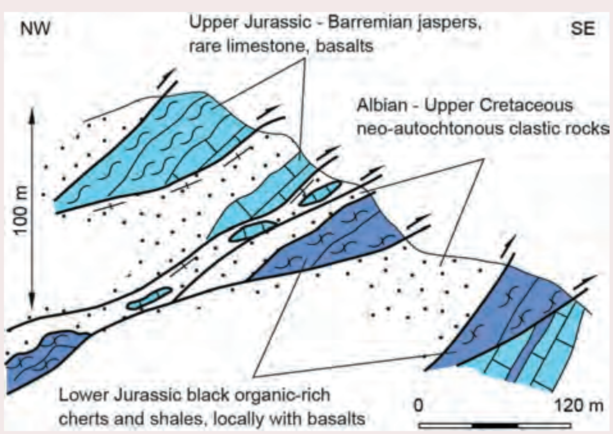


**ARTICLE HISTORY**
Received 5 November 2020
Accepted 8 November 2020

**KEYWORDS**
Lower Jurassic-Cretaceous clayey radiolarites successions; organic-rich black shales and cherts; euxinic deep water settings; Koryak-Western Kamchatka orogenic belt; Paleo-Pacific Ocean

## Introduction

The composition, depositional, and diagenetic environments of many lithological facies including siliceous and black shales associations are strongly affected by many factors, including type of sedimentary basin (epi-continental, marginal, or intra-oceanic), geochemistry of the water column, water temperature, and global climate changes. Additional factors affecting the accumulation of siliceous rocks involve changes in water level, topography, extent of erosion and rock composition of the landscapes surrounding sedimentary basins (Gavrilov 1989). The volcanic and hydrothermal activity influences the geochemical balance and temperature of marine water (Palfy and Smith 2000; Bailey *et al*. 2003; Bond and Wignall 2014; Bougeault *et al*. 2017). The combination of these factors determines the degree of oxygen in the water column and changes of conditions from aerobic to poorly oxygenated and anoxic

**CONTACT** Elena Konstantinovskaya konstant@ualberta.ca Integrated Petroleum Geosciences, Earth and Atmospheric Sciences, 1-26 Earth Sciences Building, University of Alberta, Edmonton, Alberta T6G 2E3, Canada

and ultimately euxinic (i.e. sulfidic) settings (Jenkyns 1988, 2010; Gavrilov *et al*. 2002; Kholodov 2002; Kemp and Izumi 2014; Arabas *et al*. 2017). The global Toarcian oceanic anoxic event (T-OAE) represents perturbations in marine biotic associations, fluctuations in isotope and geochemical systems of the water column, and development of organic-rich black shales, as was shown for Mesozoic basins of Tethys (Jenkyns 1988, 2010; Farrimond *et al*. 1994; Palfy and Smith 2000; Jenkyns *et al*. 2002; Hesselbo *et al*. 2007; Gomez *et al*. 2008; Arabas *et al*. 2017; Bougeault *et al*. 2017) and the Paleo-Pacific (Caruthers *et al*. 2011; Grocke *et al*. 2011). At the same time, it was shown that even though similar multiple perturbations of carbon isotope cycles and associated parameters occurred in the Early Jurassic (Storm *et al*. 2020), not all of them could be identified as global-scale events (Westermann *et al*. 2010).

Data on composition and depositional environments of Jurassic-Lower Cretaceous (Barremian) siliceous sedimentary successions in orogenic belts of the Pacific area are rather limited (Hori 1992, 1997; Matsuoka *et al*. 1996; Kemkin and Kemkina 2004, 2015; Hori *et al*. 2007; Jenkyns 2010; Wignall *et al*. 2010; Ikeda *et al*. 2018). Sedimentary units of the same stratigraphic interval are poorly characterized in the remote areas of northeastern Asia. Only fragments of Mesozoic oceanic crust that originated in the Paleo-Pacific Ocean are preserved in present-day tectonic structures of the northwestern continental margin of the Pacific Ocean (Nokleberg *et al*. 1994; Sokolov *et al*. 1996, 2003; Filatova 1998). Depositional environments of siliceous sedimentary successions are discussed for a variety of types of sedimentary paleo-basins (Jenkyns and Winterer 1982; Grocke *et al*. 2011). Allochthonous Jurassic-Lower Cretaceous siliceous rocks are recognized over a vast region in the Middle Cretaceous Koryak-Western Kamchatka orogenic belt (Filatova 2014, 2018) in the northwest tectonic framework of the Pacific Ocean (Figure 1). These rocks locally occur in association with volcanic rocks of mid-oceanic ridge basalt (MORB-), within-plate basalt (WPB-), oceanic island basalt (OIB-) types (Berezner *et al*. 1990; Filatova *et al*. 1990; Filatova and Vishnevskaya 1994; Filatova 1998; Konstantinovskaya 1998; Bogdanov *et al*. 2003; Sokolov *et al*. 2003; Khanchuk *et al*. 2006; Bondarenko *et al*. 2008). Previous study of radiolarian microfossil assemblages helped to determine the age of the siliceous rocks and allowed detailed stratigraphic correlation of Jurassic-Lower Cretaceous successions that are preserved in the imbricated tectonic structures of the Koryak-Western Kamchatka orogenic belt (Vishnevskaya 2001; Vishnevskaya and Filatova 2008, 2012).

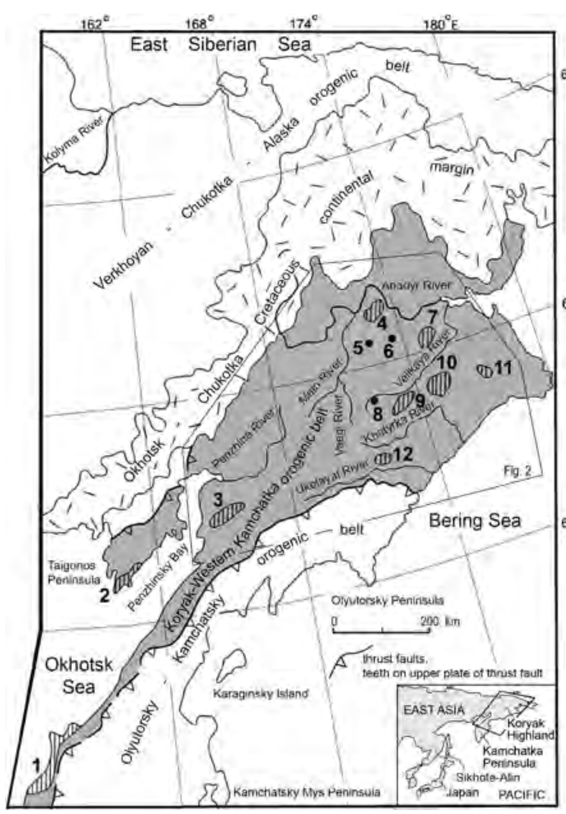


**Figure 1.** Location of allochthonous Jurassic-Lower Cretaceous marine siliceous, siliceous-volcanic and associated rocks in Middle Cretaceous Koryak-Western Kamchatka orogenic belt at the northwestern continental margin of the Pacific Ocean, modified after (Vishnevskaya and Filatova 2012). Numbers indicate geographic locations shown in Figures 3–5. Inset map shows the location of the study area.

Analysis of radiolarian assemblages was used to reconstruct paleo-temperature conditions in Paleo-Pacific water columns (Vishnevskaya and Filatova 2017).

The present study aims to characterize stratigraphic location, structural position, areal distribution, specific facies, and depositional environments of allochthonous Jurassic-Lower Cretaceous siliceous rocks and black organic-rich shales of the Koryak – Western Kamchatka orogenic belt (Figure 1). Volcanic rocks locally associated with the siliceous rocks are briefly described. In particular, composition and regional distribution of Sinemurian-Toarcian units of pelagic black organic-rich cherts and shales in this region are analysed in detail for the first time. The study synthetizes the original data collected by the author during many years of field work in East Asia. Comparative analysis of allochthonous Jurassic-Lower Cretaceous siliceous rock and black shale associations from the study area and fold-and-thrust belts of Japan and Sikhote-Alin located in East Asia to the northwest of Japan (Figure 1, inset map) is used to infer palaeogeographic settings of these rocks.

## Methodology

Jurassic-Barremian allochthonous marine lithotectonic complexes of tectono-stratigraphic sections of the Koryak-Western Kamchatka orogenic belt are characterized on the basis of stratigraphic analysis of radiolarians and comparative lithological and facies analysis of restored stratigraphic successions. Detailed stratigraphic study of radiolarian microfossils extracted from siliceous rocks of allochthonous lithotectonic complexes of the Koryak-Western Kamchatka orogenic belt helped to determine the age of sedimentary successions from individual tectonic slices (Vishnevskaya and Filatova 2008, 2012, 2017). The lithotectonic units were sampled continuously along transverse lines across the key areas of stacked tectonic slices. The thinnest of these stratigraphic units and the highly imbricated tectonic structure of the study region required high-density sampling to carry out stratigraphical and lithological correlation of rock units from discrete tectonic slices. Petrographic and geochemical studies (Zlobin *et al*. 1992; Filatova and Vishnevskaya 1994) with the help of detailed age data (Vishnevskaya and Filatova 2016, 2018) were conducted to identify and characterize specific facies within lithotectonic complexes from different areas of the study region.

## Geologic settings

The Jurassic-Lower Cretaceous (Barremian) allochthonous lithotectonic complexes form thin tectonic slices in the imbricated tectonic structure of the Middle Cretaceous Koryak – Western Kamchatka orogenic belt over a large area (Figure 1) that extends along the northwestern margin of the Pacific Ocean (Filatova 2018). The main deformation phase of the belt is dated as late Aptian-early Albian (Filatova 1998, 2014). Albian-Upper Cretaceous neoautochthonous cover of clastic rocks overlies with angular unconformity the fold and thrust structure of the belt (Figure 2). Jurassic-Lower Cretaceous allochthonous lithotectonic complexes include marine oceanic, back-arc basin, and island-arc rocks that have been accreted to the continental margin during mid-Cretaceous orogeny. Both Jurassic-Lower Cretaceous allochthonous thrusts and nappes and Albian-Upper Cretaceous parautochthonous rocks were subsequently deformed during the emplacement of the Olyutorsky – Kamchatsky orogenic belt in the Early Eocene (Figure 2).

In the present-day tectonic structure of the Koryak-Western Kamchatka orogenic belt, allochthonous Jurassic-Early Cretaceous (Barremian) siliceous and basalt-bearing rock associations compose thin tectonic slices differentially displaced by thin bedding-parallel detachments and refolded in antiformal and synformal stacked structures, in which fragments of rock successions of different age and composition are superimposed (Figure 3). The allochthonous tectonic slices of Jurassic-Lower Cretaceous complexes on the Nauchirynay River (Figure 3(a)) form a series of folded nappes emplaced over mafic-ultramafic rocks and serpentinite melange in the core of the Yagelnaya Antiform. The upper nappe consists of stacked, often repeated, alternation of tectonic allochthonous slices of the Triassic-Jurassic-Hauterivian rocks. Core zones of synforms are composed of tectonic slices of Lower Jurassic black cherts and shales with lenses and slices of basalts of the MORB- and WPB-types and Middle Jurassic siliceous rocks. Tectonic structure of the Koyverelan River area and the Semiglavaya Mount (Figure 3(b)) represents a large synform composed of imbricated slices of allochthonous and parautochthonous lithotectonic complexes. At the outcrop scale, Lower Jurassic radiolarian-bearing organic-rich black cherts and Upper Jurassic-Barremian haematitic jaspers and limestone form packages of tectonic slices of various thicknesses from a few metres to 10–30 m imbricated with parautochthonous rocks (Figures 3(c,d)).

Thrusting and folding of Middle Mesozoic allochthonous marine lithotectonic complexes in the Koryak-Western Kamchatka orogenic belt occurred in the Aptian-early Albian (Filatova 1998, 2014), synchronously with accretionary and collisional tectonic processes along the western and eastern continental margins of the Pacific (Gursky and Schmidt-Effing 1982; Matsuoka *et al*. 1996; Struik *et al*. 2001; Caruthers *et al*. 2011; Kemkin and Filippov 2011).

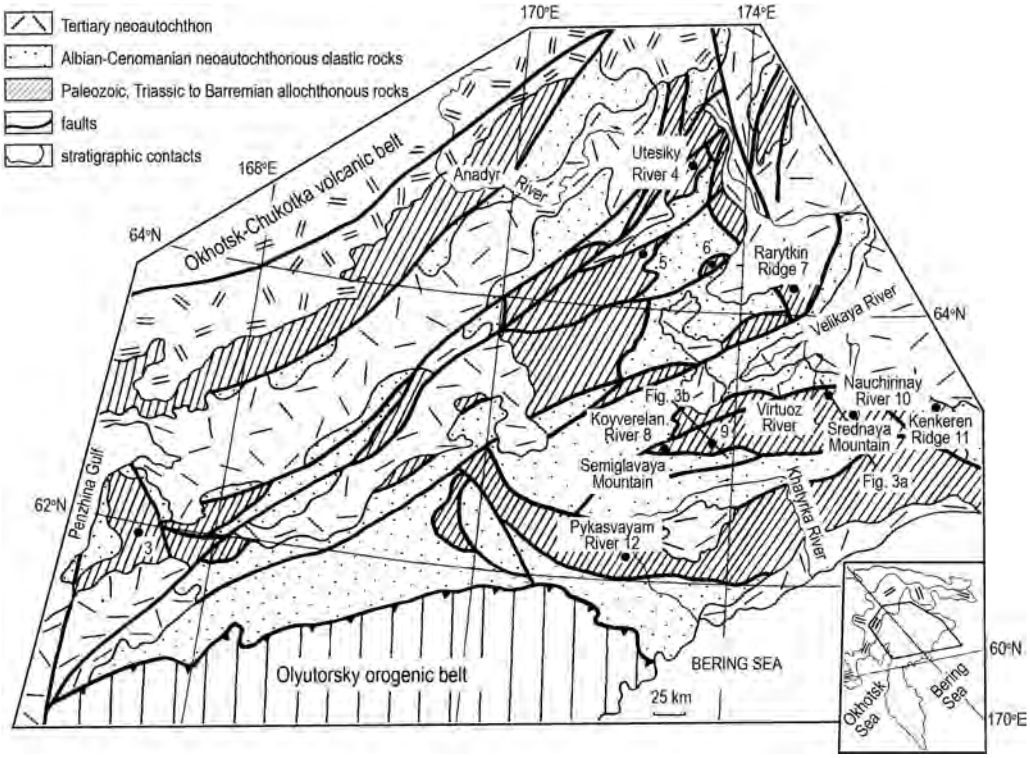


Figure 2. Map of allochthonous Jurassic-Lower Cretaceous terranes in the Koryak orogenic belt, modified after (Filatova and Vishnevskaya 1997). Numbers and black dots indicate geographic locations of columns shown in Figures 4–5. The inset map shows location of the area in East Asia.

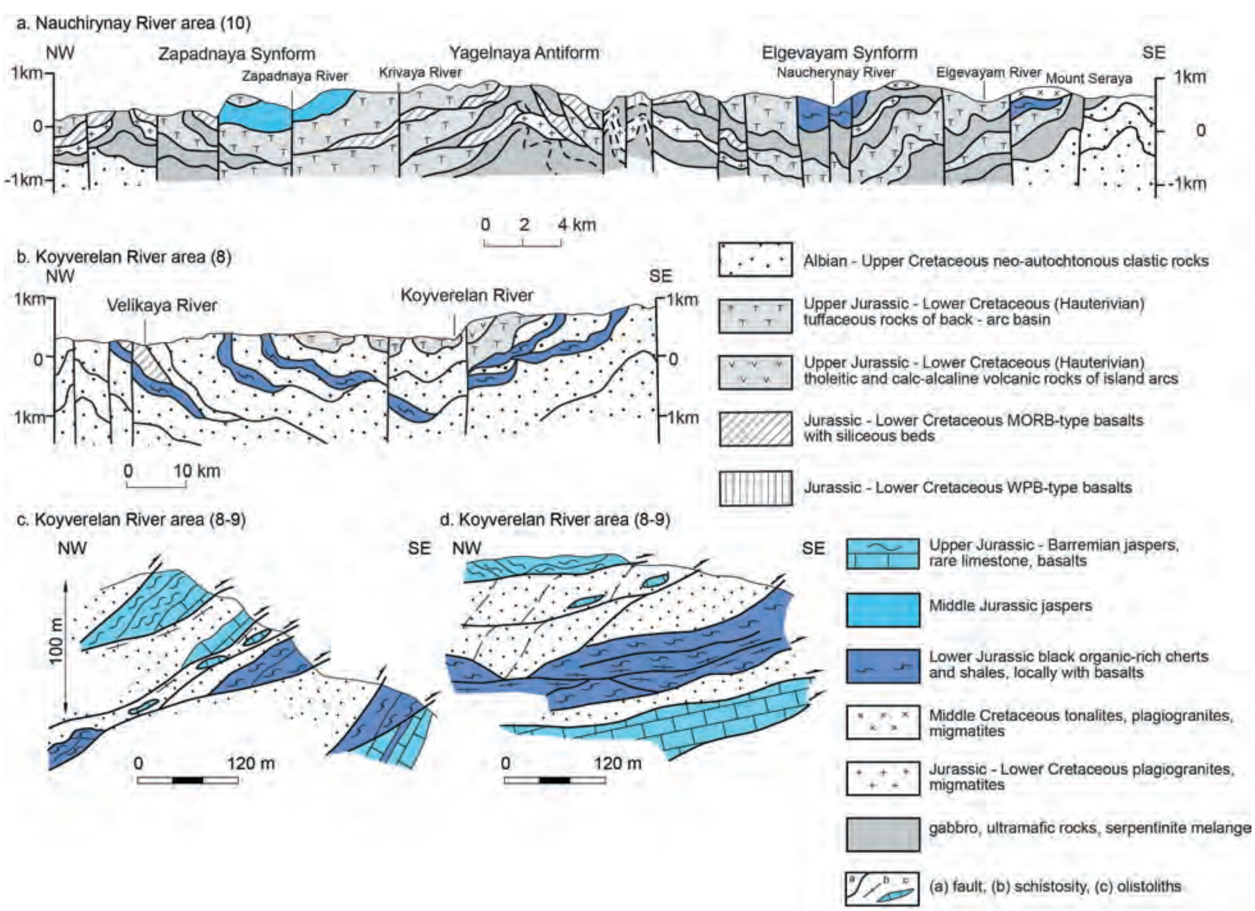


Figure 3. Structural cross-sections and outcrops of the allochthonous Jurassic–Lower Cretaceous complexes of the Koryak orogenic belt. See Figure 2 for location of the cross-sections.

## Jurassic-Lower Cretaceous siliceous rocks of the Koryak-Western Kamchatka orogenic belt

Jurassic–Lower Cretaceous (Barremian) allochthonous marine lithotectonic complexes have been identified and samp led in different tectono-stratigraphic sections of the Koryak-Western Kamchatka orogenic belt (Figure 2). Siliceous rock units are composed of haematitic jaspers (Hettangian and Aalenian–Barremian) and Sinemurian-Toarcian pyrite-bea ring organic-rich black cherts and siliceous shales (Figure 4, type 1). Additionally, Jurassic-Lower Cretaceous jasper and cherts are present in association with basalts of MORB- and WPB-types (Figure 4, type 2). Less abundant are siliceous rocks intercalated with tuffaceous, volcaniclastic, and volcanic rocks of back-arc basins (BAB) type (Figure 4, type 3).

The stratigraphic successions in the studied areas are reconstructed from imbricated tectonic slices with the help of age determinations of radiolarian assemblages and individual index-species (Figure 4). In total, 20 radiolarian complexes of different ages from the Lower Jurassic (Hettangian) to Lower Cretaceous (Barremian) have been identified in marine siliceous and siliceous-basaltic successions (Vishnevskaya 2001; Vishnevskaya and Filatova 2008, 2012) and correlated with the North America radiolarian zones of Cordey (1998), Pessagno and Martin (2003) and Pessagno *et al*. (1993); (2009).

### Jurassic-Lower Cretaceous siliceous successions

#### Lower Jurassic

Lower Jurassic siliceous rock units (type 1) are restored in a continuous succession from Hettangian to Toarcian. Lower Hettangian red jaspers with corresponding index-species of radiolarians crop out in the Nauchirynay River area (Figures 2, 4, section 10). The Lower Hettangian unit (40 m thick) is composed of red jaspers with subordinate WPB-type basalts that form an upper tectonic slice in this area (Figure 5(a)). The Upper Hettangian to Lower Sinemu rian unit is exposed in a lower tectonic slice and represents a continuous succession of siliceous rocks about 115 m thick (Figure 5(a)) that contains radiolarian assemblages of two different ages (Figure 4). Upper Hettangian rocks consist of thinly laminated haematitic jaspers with rare thin lenses of organic-rich cherts. Lower Sinemurian rocks are

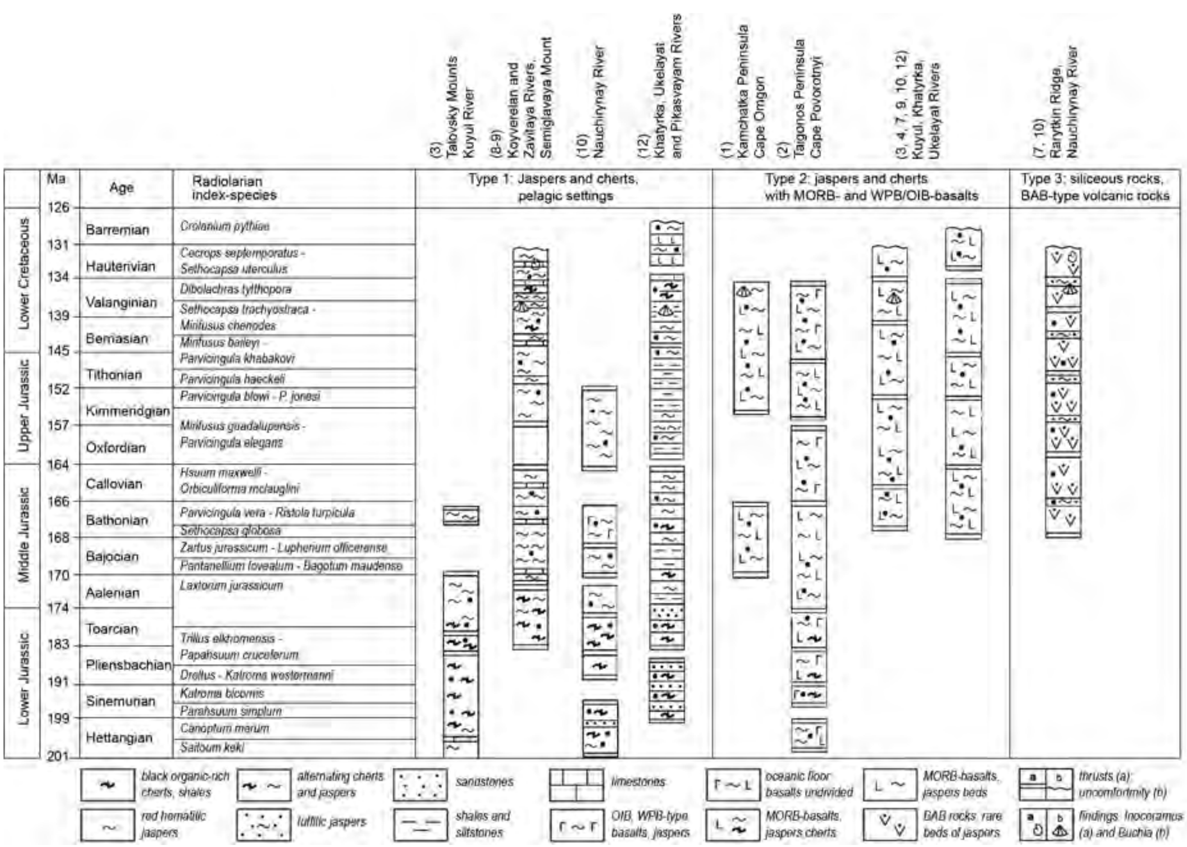


Figure 4. Restored stratigraphic successions of allochthonous Jurassic–Lower Cretaceous lithotectonic complexes of the Koryak-Western Kamchatka orogenic belt. The numbers above the sections correspond to locations shown in Figure 1, 2. Black dots indicate sampling location of radiolarian assemblages.

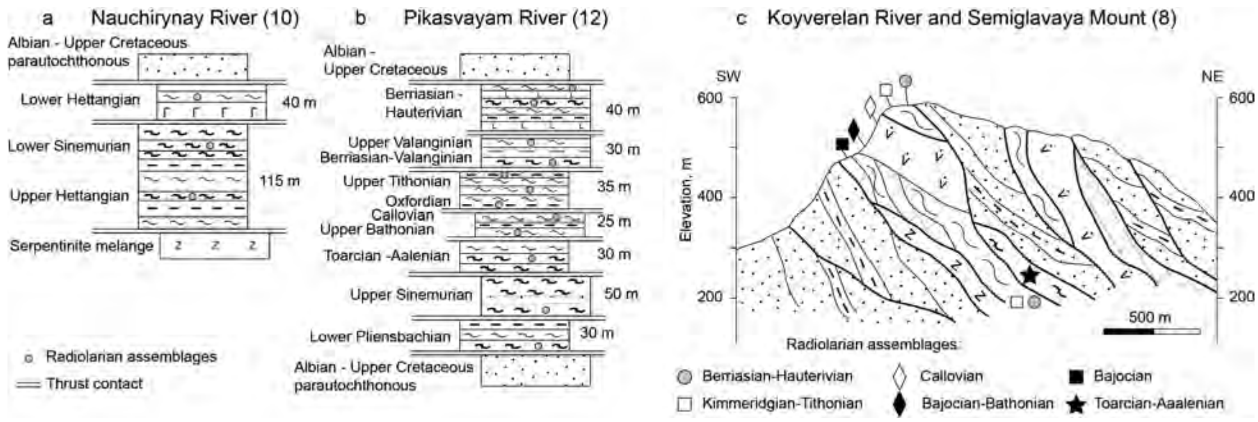


**Figure 5.** Imbricated tectonic structure of the allochthonous Jurassic–Lower Cretaceous lithotectonic complexes exposed in outcrops of the Koryak orogenic belt. Age of rocks is determined from radiolarian assemblages (Vishnevskaya and Filatova 2008, 2012). See Figures 1 and 2 for the outcrop location and Figure 4 for the lithology symbols.

composed of organic-rich thinly laminated black cherts with beds of volcaniclastic sandstones and siltstones. The black unstructured organic matter is present in these rocks as very thin microlayers, lenses, or isometric agglomerations in a fine-grained chalcedony matrix (Figure 6(a,b)). Abundance of radiolarian and sponge fragments in the rocks may indicate marine planktonic and probably bacterial origin of organic matter. Pyrite enrichment characterizes some layers. Lower-Upper Hettangian and Lower-Upper Sinemurian index-species of the region (Figure 4) can be correlated in age with their analogs of zones 05–03 in British Columbia (Carter *et al*. 1998; Cordey 1998) and California and Mexico (Pessagno *et al*. 1993; Pessagno and Martin 2003).

Black siliceous rocks with index-species of Upper Sinemurian – Lower Pliensbachian radiolarians (Figure 4) are present in the Pikasvayam area (Figures 2, 4, section 12). A tectonic slice of Lower Pliensbachian rocks is composed of a rhythmic alternation of black and dark-grey pyrite-bearing organic-rich cherts, cherty shales, and siliceous siltstones with a total thickness of 30 m (Figure 5(b)). A structurally higher tectonic slice of Upper Sinemurian rocks is about 50 m thick and consists of black organic-rich cherts with beds of siltstones and mudstones. Individual beds of thinly laminated cherts are up to 5–7 m thick. A Lower Jurassic siliceous rocks unit (60 m thick) in the area of the Talovsky Mountains and the watershed of the Kuyul River (Figure 2, section 3) contains predominantly grey organic-rich cherts with subordinate siliceous shales and siltstones bearing Late Sinemurian and Early Pliensbachian radiolarians (Figure 4, section 3) (Khanchuk *et al*. 1990, 1992, 2006; Vishnevskaya 1994, 2001). Pliensbachian index-species (Figure 4) are correlated with high confidence (Vishnevskaya and Filatova 2012) with their age analogs in British Columbia that also contain ammonites, and with zone 02 in California and Mexico (Pessagno *et al*. 1993; Pessagno and Martin 2003). They are in good stratigraphic correlation with the well-dated radiolarian pelagic cherts of Pliensbachian and possibly early Toarcian age from the Cache Creek Terrane of the Canadian Cordillera due to presence of *Atalantria epaphrodita* Cordey et Carter, *Praeconocaryomma decora* gr.,*Bipedis* sp. (Cordey 2020).

The Toarcian unit is composed of micro-laminated organic-rich black radiolarites, cherts, and shales and is 30–40 m thick. The unit is widely present in the study area (Figure 2, sections 3, 8–9, 10–12) and locally forms a continuous succession with Aalenian jaspers in tectonic slices of the Pikasvayam River (Figure 5(b)) and Koyverelan River (Figure 5(c)). The index-species of radiolarians of the unit correspond to Toarcian analogs of the Canadian Cordillera (Cordey 1998), while Toarcian and Aalenian radiolarians in California and Mexico are considered to form a single zone 1A (Pessagno *et al*. 1993; Pessagno and Martin 2003).

## Middle Jurassic

The most complete and stratigraphically continuous Middle Jurassic siliceous succession is recognized in tectonic slices of the Velikaya and Koyverean Rivers area, Koryak Highland (Figure 2, sections 8–9), as well as of the Omgon Cape of Kamchatka. Aalenian-Callovian units 40 m thick consist of haematitic red jaspers and rare organic-rich bioclastic limestone. Bajocian, Bathonian, and Callovian radiolarian assemblages (Figure 4, sections 8–9) are correlated with high confidence (Vishnevskaya and Filatova 2012) with their age analogs in the Canadian Cordillera (Cordey 1998, 2020), California and Mexico, zones 1B-1 H (Pessagno *et al*. 1993; Pessagno and Martin 2003), and in some parts of Japan (Matsuoka *et al*. 1996). Based on the taxonomic composition of radiolarians, they also correlate well with the oldest Bathonian-Callovian reliably established radiolarian cherts (Matsuoka 19

92) in the basal sedimentary strata of Site 801 in the Pacific Ocean in the central Pigafetta Basin (18°38.54′N, 156°21.58′E) (Ogg *et al*. 1992a). Middle Jurassic rocks form a mesoscopic antiform that is exposed in the Semiglavaya Mount and Koyverelan River area (Figure 2, section 8). The imbricated tectonic slices, 20 m thick (Figure 5(c)) are composed of Bajocian jaspers with interlayers of limestones, Bajocian-Tithonian tuffaceous rocks and Kimmeridgian-Hauterivian deep-water haematitic jaspers. In the Pikasvayam River area (Figure 2, section 12), Bathonian – Callovian jaspers are rhythmically intercalated with layers of siliceous shales (Figure 5(b)), forming a unit 25 m thick.

### *Upper Jurassic – Lower Cretaceous (Barremian) succession*

Kimmeridgian-Hauterivian radiolarian-bearing siliceous rocks (Figure 4, type 1) form relatively thick (80 m) and continuous unit in the Koyverelan River area (Figure 2). The lower Upper Kimmeridgian-Tithonian part of the unit (20 m) is composed of laminated red and greyish-green jaspers (Figure 4, section 9). The middle Tithonian-Berriasian part of the unit (30 m) consists of alternating red jaspers and pink calcareous jaspers that are replaced upward by pinkish-grey siliceous limestone. The radiolarian association in the Tithonian chert alternating with limestone in the Nauchirynai and Semiglavaya areas of the Koryak Highland is very close to the radiolarian association in the chert of the same age of Site 305 at the Shatsky Rise, northwestern Pacific Ocean (Basov and Vishnevskaya 1991). The upper Berriasian-Valanginian part of the unit (30 m) is composed of jaspers, calcareous jaspers, cherts, and siliceous limestone. The rocks from the uppermost part of the unit contain the Valanginian-Hauterivian radiolarian index-species *Cecrops septemporatus* (Figure 4) that is characteristic of the uppermost Hauterivian pelagic rocks of Italy (Cecca *et al*. 1993). The age of the succession is based on radiolarian assemblages extracted from the siliceous rocks. Siliceous limestone in the upper part of the succession contains bivalves of Valanginian – Lower Hauterivian age (*Buchia cf. inflata* and *B. cf. sibirica* (Terekhova and Shmakin 1982)), and Hauterivian age (*Inoceramus colonicus Fnd*. and *I. heteropteris Poch*. (G.P. Terekhova, pers.comm.)).

Oxfordian-Kimmeridgian thinly layered jaspers are recognized in tectonic slices of the Nauchirynay River (Figure 2), where they form units 15–20 m thick (Figure 4, section 10). Oxfordian-Barremian siliceous rocks about 100 m thick were identified in the Ukelayat and Pikasvayam Rivers area (Figures 2, 4, section 12). This succession is reconstructed from a package of tectonic slices each 30–40 m thick (Figure 5(b)), and it is mostly composed of haematitic jaspers and siliceous shales with rhythmic bedding, locally enriched by haematitic and Fe-hydroxides (Figure 6(c)). Lenses of pillow basalts and beds of black shales are present in the Berriasian-Valanginian unit, and basalt lavas are typical of the Hauterivian-Barremian unit (Figures 4, 5(b)).

Upper Jurassic radiolarian assemblages are similar (Vishnevskaya and Filatova 2012) to radiolarian associations from zones 2, 3 and 4 of California and Mexico, while Berriasian – Valanginian ones are correlated with their analogs from zones 5A, 5B, 5C and Hauterivian and Barremian radiolaria correspond to zone 6 (Pessagno *et al*. 1993, 2009; Pessagno and Martin 2003).

Jurassic – Lower Cretaceous radiolaria-bearing siliceous rocks are also present in the form of lenses associated with volcanic rocks of MORB- and WPB-types (Figure 4, type 2). The Lower Hettangian unit with corresponding index-species of radiolarians (Figure 4, section 2) crops out on the Taigonos Peninsula (Figure 1). It is composed of red jaspers and MORB-type basalts. Black organic-rich cherts and siliceous shales containing Sinemurian and Pliensbachian index-species (Kemkin *et al*. 1996; Chamov and Andreev 1997; Vishnevskaya *et al*. 1998) are recognized in the south-western part of the peninsula (Figure 1, section 2), where they (Figure 4) are associated with basalts of OIB- and MORB-types (Konstantinovskaya 1998; Bondarenko *et al*. 2008). Toarcian black cherts and shales and Aalenian haematitic jaspers contain lenses of basalts of MORB- and WPB-type on the Taigonos Peninsula (Figures 1, 4, section 2).

Middle Jurassic jaspers and cherts are present as lenses and inter-pillow irregular filling in pillowed flows of basalts of the MORB- and OIB-types. Volcanic and siliceous units in the Cape Omgon area of Western Kamchatka (Figure 1, section 1) are dated as Bajocian-Bathonian (Vishnevskaya *et al*. 1998; Vishnevskaya 2001). These units are composed of MORB-type pillow lavas, jaspers, and siliceous shales (Bogdanov *et al*. 2003). In other areas (Figures 1, 5, sections 2, 3, 10), Bajocian, Bathonian, and Callovian siliceous rocks are associated with basalts of MORB- and OIB-type (Khanchuk *et al*. 1992; Konstantinovskaya 1998; Bondarenko *et al*. 2008).

The Upper Jurassic-Lower Cretaceous (Barremian) interval is also characterized by thick units composed of jaspers and basalts. MORB-type basalts with lenses of jaspers and cherts with a total thickness of 120 m (Figure 4, section 12) are exposed in the Khatyrka River and Ukelayat River areas (Figure 2) (Ruzhentsev *et al*. 1982; Peyve 1984). Similar units are known in the area of the Main and Anadyr Rivers and in the Nauchirynay River area (Figures 2, 4, sections 4–6, 10, 11) (Berezner *et al*. 1990; Zlobin *et al*. 1992; Filatova and Vishnevskaya 1994). Oxfordian-Hauterivian jaspers and basalts of MORB- and OIB-types (Figure 4, sections 2–3) are exposed in the Taigonos Peninsula and in the Kuyul

River area (Khanchuk *et al*. 1992; Sokolov *et al*. 1996, 2003; Konstantinovskaya 1998; Bondarenko *et al*. 2008). N-MORB-type basalts with lenses of Kimmeridgian-Valanginian jaspers (Figures 2, 4, section 1) are present in the tectonic structure of the Omgon Peninsula, Western Kamchatka (Vishnevskaya *et al*. 1998; Vishnevskaya 2001; Bogdanov *et al*. 2003).

Rare beds of Middle Jurassic and Upper Jurassic–Lower Cretaceous radiolarian-bearing tuffaceous siliceous rocks (Filatova *et al*. 1990; Krymsalova 1994; Vishnevskaya and Filatova 2012) are recognized in thick (up to 600 m) back-arc basin successions (Figure 4, type 3) in the Velikaya, Koyverelan, Nauchirynay, and Pikasvayam Rivers area (Figures 2, 4, 5). The tuffaceous units in the Koyverelan River area contain Callovian ammonites (Terekhova and Shmakin 1982). Tuffaceous rocks of the Rarytkin Range and the Nauchirynay River (Figure 2) contain Valanginian *Buchia* and Hauterivian *Inoceramus colonicus* (K.V. Paraket sov, G.I. Paraketsova, pers. comm.).

## Geochemical composition of the Triassic And Jurassic-Lower Cretaceous siliceous rocks of the East Asia

The geochemical composition of the Upper Triassic and Jurassic–Lower Cretaceous siliceous formations of the East Asia is characterized in the Taigonos Peninsula (Kon stantinovskaya 1998), Kuyul area (Grigor'ev *et al*. 1995) and Sikhote-Alin area (Volokhin *et al*. 2005; Volokhin and Ivanov 2007; Volokhin 2013) (Figure 1) and compared to the Middle Jurassic – Valanginian radiolarites and mudstones of Sites 800 and 801 drilled on ODP Leg 129 (Ogg *et al*. 1992a, 1992b).

The siliceous rocks from imbricated tectonic slices of the Taigonos Peninsula are dated from Upper Triassic to Lower Cretaceous (Figure 4, section 2) and contain rhythmic-layered biogenic silica-rich radiolarites, radiolarian jaspers and siliceous claystones, locally apatite-bearing (TJC1), with subordinate amounts of Fe- and Mn-rich haematitic jaspers, carbonaceous jaspers and carbonate rocks associated with MORB-type basalt pillow crusts (TJC2). The siliceous rocks form a continuous tre nd (Figure 7(a)) from deposits rich in biogenic silica ($SiO_2$ 88–95%) to siliceous claystones with $SiO_2$ 58–70% and aluminium component Al/(Al+Mn+Fe) larger than 0.5, similar to the trends in Cenozoic open pelagic deposits of the Pacific Ocean (OPD) and Philippine Sea (PSD) (Svalnov and Gordeev 1986). The silica-rich radiolarites are characterized by relative enrichment in intermediate REE normalized to Post-Archaean Australian Shale (PAAS) (McLennan and Taylor 1981) and strong negative Ce anomaly (Figure 7(b)), similar to deep ocean water (DOW) (Klinkhammer *et al*. 1983) and deep-seawater pelagic deposits in the Pacific (Hein *et al*. 1993). Claystones and clay-rich radiolaria-bearing siliceous rocks are characterized by flat PAAS-normalized REE distribution (Figure 7(b)), similar to those observed in pelagic clay rocks. The $TiO_2$ value is the lowest (0.1) in the Upper Triassic radiolarite and it ranges from 0.16% to 0.36% in the silica-rich radiolarites to 0.51–0.98% in the carbonaceous jaspers and clay-rich siliceous rocks (Figure 7(c)). The (Fe+Mn)/Ti ratio varies from 7 to 19 in the Jurassic-Lower Cretaceous siliceous rocks to 27 in the Upper Triassic radiolarite (Figure 7(d)).

The Jurassic-Lower Cretaceous Fe- and Mn-rich haematitic jaspers ($SiO_2$ 87–89%) and carbonates ($SiO_2$ 22%) of the Taigonos Peninsula are associated with bas alt pillow crusts, inter-pillow spaces or forming interlayers in the radiolarites. The Fe-Mn haematitic jaspers are characterized by low Al/(Al+Mn+Fe) component 0.-06–0.14 (Figure 7(a)), low $TiO_2$ (0.1–0.21%) (Figure 7(c)) and elevated (Fe+Mn)/Ti ratio ranging 27–39 (Figure 7(d)). The Fe-Mn-rich carbonate has higher Al and Ti com ponents and lower (Fe+Mn)/Ti ratio compared to the haematitic jaspers (Figures 7(c-d)). The Fe-Mn-rich haematitic jaspers and carbonates are characterized by differentiated REE distribution with LREE depletion (Figure 7(b)), identical to those in associated MORB-type basalts (Konstantinovskaya 1998). The radiolarian jaspers with manganese nodules have a differentiated REE distribution with positive Ce anomaly (Konstantino vskaya 1998), similar to hydrogenic ferromanganese crusts in Tertiary sediments of the Pacific (Bau *et al*. 1996). The microglobular Fe-rich haematitic jaspers form ing interlayers among radiolarites have LREE-enriched PAAS-normalized distribution (Figure 7(b)), similar to high-temperature hydrothermal solutions of the East Pacific Rise (Michard *et al*. 1983).

The Triassic (SAT) and Middle-Upper Jurassic (SAJ) siliceous rocks of the Sikhote-Alin area vary in composition from radiolarian cherts to siliceous claystones (Volokhin 2013) and form two distinct trends on the diagram $SiO_2$ vs Al/(Al+Mn+Fe) component (Figure 7(a)). The Jurassic rocks are similar in composition to the Jurassic-Lower Cretaceous siliceous rocks of the Taigonos Peninsula, while the Triassic rocks of the Sikhote-Alin area have higher silica content than the Jurassic rocks of the same aluminium component (Figure 7(a)). The Lower-Middle Triassic (Upper Olenekian to Upper Anisian) cherts, carbonaceous cherts, and argillites of the Sikhote-Alin area are organic-rich and contain 0.3 to 8.5 wt. % $C_{org}$ that form a unit of 4–20 m thick (Volokhin and Ivanov 2007). The slightly oxidized organic (primarily, marine sapropelic) matter contains quinones, methyl, methylene, and ether groups. The content of neutral bitumens in rocks shows a wide variation range. The carbon isotopic composition

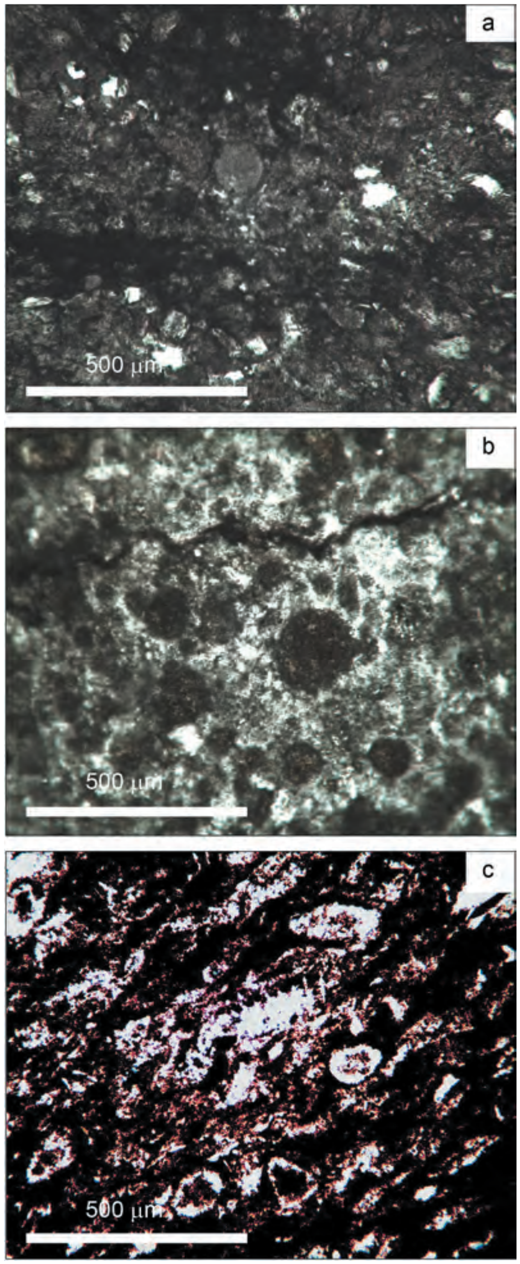


**Figure 6.** Microphotographs of Jurassic – Lower Cretaceous siliceous rocks from allochthonous complexes of the Koryak Highland, East Asia, plane polarized light. a, Lower Jurassic black chert with organic-rich microbeds in siliceous matrix and Radiolarian remnants (white debris and grey round fragments); b, Lower Jurassic black chert, variably organic-rich, with Radiolarian remnants (grey round fragments); c, Jurassic – Lower Cretaceous Radiolarian red jasper.

($\delta^{13}C$) in organic-rich siliceous rocks varies from −27.3 to −30.2‰ that is identical to composition of many Palaeozoic-Mesozoic bitumens and oils (Volokhin *et al.* 2005). The carbonaceous siliceous rocks are enriched in V, B, Mo, Ni, Cu, and Ag, As, and locally in Ba, compared to other Mesozoic sedimentary rocks of the Sikhote-Alin area. The organic-rich shales with $C_{org}$ >0.5% are characterized by positive Au-$C_{org}$ correlation.

The Middle Jurassic-Lower Cretaceous (Bathonian-Valanginian) sedimentary rocks analysed in Sites 800 and 801 in the Pacific Ocean contain clayey radiolarites (from biogenic silica-rich to clay-rich layers), Fe- and Mn-rich radiolarites, Fe-rich claystone and calcite-rich metalliferous radiolarite associated with basal pillows (Ogg *et al.* 1992b). The biogenic silica-rich and clay-rich radiolarites rocks are characterized by Al/(Al+Fe+Mn) ratio (0.34–-0.69), that is lower (0.11–0.24) in the Fe- and Mn-rich pillow crusts (Figure 7a). The radiolarites have lower content of silica ($SiO_2$ < 74%), with exception for radiolarian clusters ($SiO_2$ 93%) (Figure 7a), lower content of $TiO_2$

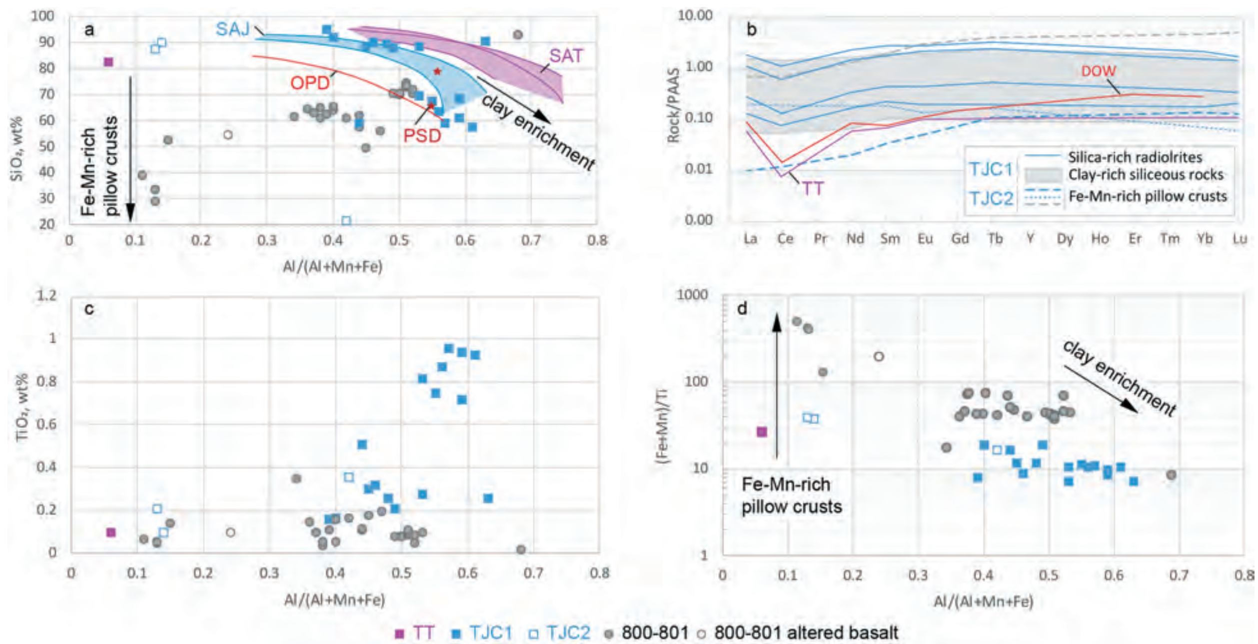


**Figure 7.** Geochemical composition of siliceous rocks of East Asia and Pacific area. In letters: TT, Triassic radiolarite; TJC1, Jurassic-Lower Cretaceous silica-rich radiolarites and siliceous claystones; TJC2, Fe-Mn-rich jaspers and carbonates associated with basalt pillow crusts of the Taigonos Peninsula, after Konstantinovskaya (1998); SAT, Triassic and SAJ, Middle-Late Jurassic siliceous rocks of the Sikhote-Alin area, after Volokhin (2013); 800–801, Bathonian-Valanginian clayey radiolarites and radiolarian cherts of Sites 801 and 800, after Ogg *et al*. (1992b); OPD, Cenozoic open pelagic deposits of Pacific and PSD, Philippine Sea, after Svalnov and Gordeev (1986); DOW, deep ocean water after Klinkhammer *et al*. (1983); REE is normalized to Post-Archaean Australian Shale (PAAS), after McLennan and Taylor (1981). In Figure 7(b), sample of Fe-Mn-rich jasper is shown by blue dashed line, microglobular Fe-rich haematitic jasper – by blue dotted line, Fe-Mn-rich carbonate – by grey dashed line. See Figure 9 for the sites location.

(mostly less than 0.2%) (Figure 7c), and higher (Fe+Mn)/Ti ratio, mostly above 38 (Figure 7d), compared to the siliceous rocks of the same age from the Taigonos Peninsula and Sikhote-Alin orogenic belts. The Fe- and Mn-rich pillow crusts of Sites 800 and 801 are very low in Al component and $TiO_2$ (Figure 7c), similar to the analogous rocks of the Taigonos Peninsula, but have higher (Fe+Mn)/Ti ratio (>100), close to the value in altered basalt (Figure 7d).

## Depositional environments of Jurassic-Lower Cretaceous siliceous rocks of the Koryak-Western Kamchatka belt

The restoration of paleo-latitude settings of allochthonous Jurassic-Lower Cretaceous siliceous rocks and black shales of the Koryak-Western Kamchatka orogenic belt is poorly constrained due to limited palaeomagnetic data. According to paleo-magnetic data from cherts of Japan (Shibuya and Sasajima 1986; Ando *et al*. 2001), sedimentation of these rocks occurred in the Triassic and Early Jurassic in the near-equatorial latitudes, between 10°N and 10°S; the rocks were then translated to the northern hemisphere. A similar paleo-latitudinal, near-equatorial location is reconstructed for accumulation of Pliensbachian-Toarcian cherts (Figure 8) of central Japan (Grocke *et al*. 2011; Ikeda *et al*. 2018). It is assumed that the near-equatorial zone was localized in the triple junction of spreading ridges of the Izanagi, Farallon and Phoenix plates (Figure 9) that are reconstructed in the Paleo-Pacific in the Early Jurassic (Scotese 1997; Muller *et al*. 2008). The Jurassic-Lower Cretaceous clayey radiolarites of Sites 800 and 801 also considered being accumulated at equatorial paleolatitudes based on high biogenic silica accumulation rates of about 200 g/cm$^2$/yr, similar to modern accumulation rate of opal in eastern equatorial Pacific (Ogg *et al*. 1992a).

By analogy to the data from Japan, allochthonous Jurassic-Lower Cretaceous siliceous successions of the Koryak-Western Kamchatka orogenic belt likely accumulated within the Izanagi-Kula plate (Figure 9) (Vishnevskaya and Filatova 2016). This suggestion is supported by the study of taxonomic composition and morphology of radiolarians shells that can be used to model paleolatitudes of radiolarian distribution for the Jurassic-Cretaceous (Pessagno and Martin 2003; Pessagno *et al*. 2009). It was found that siliceous rock associations from Jurassic-Lower Cretaceous lithotectonic units of the Koryak-

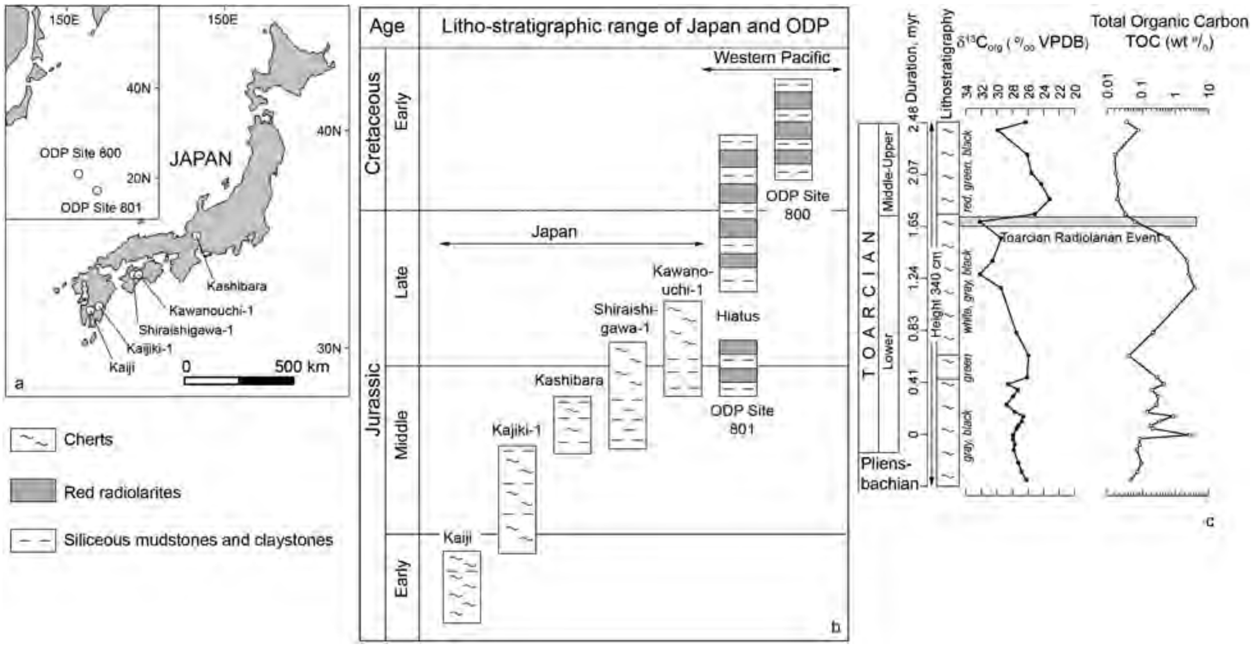


**Figure 8.** Jurassic – Lower Cretaceous radiolarian siliceous successions of Japan. (a) Location of sections; (b) lithotectonic complexes dated by radiolarian assemblages from the southwestern and central Japan, after Matsuoka (1995); (c) example of Pliensbachian – Toarcian chert succession of the Inyama area, central Japan, after Grocke *et al.* (2011). Figures 8a,b are reprinted with kind permission from John Wiley and Sons, Inc. and Figure 8c with kind permission of Dr. D. Grocke.

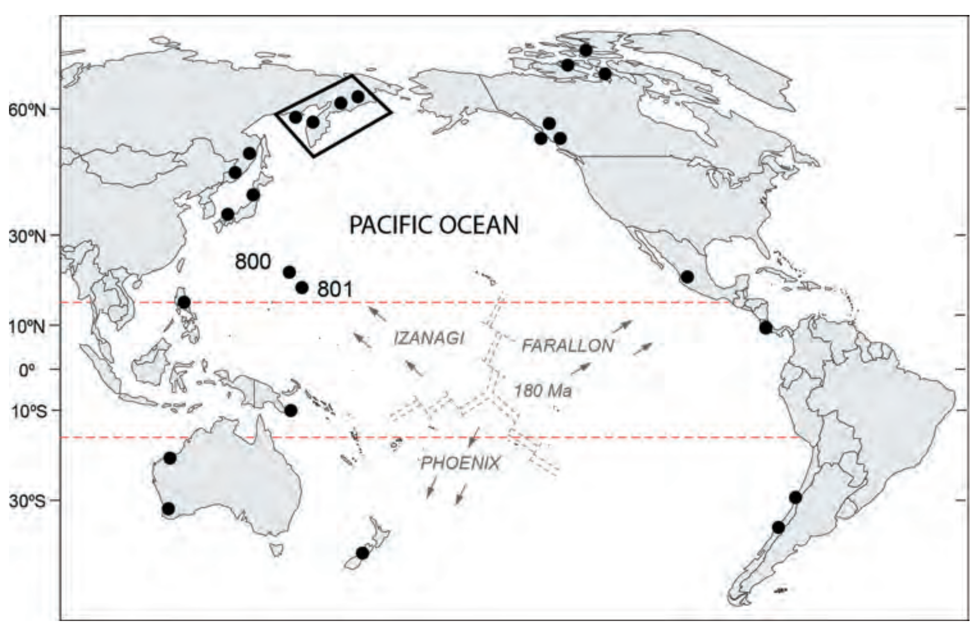


**Figure 9.** Present-day map of the Pacific region showing (i) location of Lower Jurassic (Toarcian) siliceous black shales in the Koryak-Western Kamchatka orogenic belt (polygon) and fold-and-thrust belts of continental margins of the Pacific Ocean (filled circles), based on the present study and after (Al-Suwaidi *et al.* 2016; Caruthers *et al.* 2011; Gursky and Schmidt-Effing 1982; Jenkyns 1988; Kemkin and Filippov 2011; Kemp and Izumi 2014; Marshall 2013; Matsuoka *et al.* 1996; Orchard *et al.* 2001; Robinson *et al.* 2017; Struik *et al.* 2001); (ii) Early Jurassic plate tectonic elements modified from Grocke *et al.* (2011) and Muller *et al.* (2008). Movement of tectonic plates indicated by arrows. The red dashed line shows the position of the equatorial divergence zone after Robinson *et al.* (2004).

Western Kamchatka orogenic belt contain radiolarian assemblages that accumulated at various paleolatitudes (Figure 10) that were subsequently tectonically juxtaposed in the accretionary tectonic structure of the belt (Vishnevskaya and Filatova 2017). Jurassic siliceous and siliceous-basaltic successions contain radiolarian

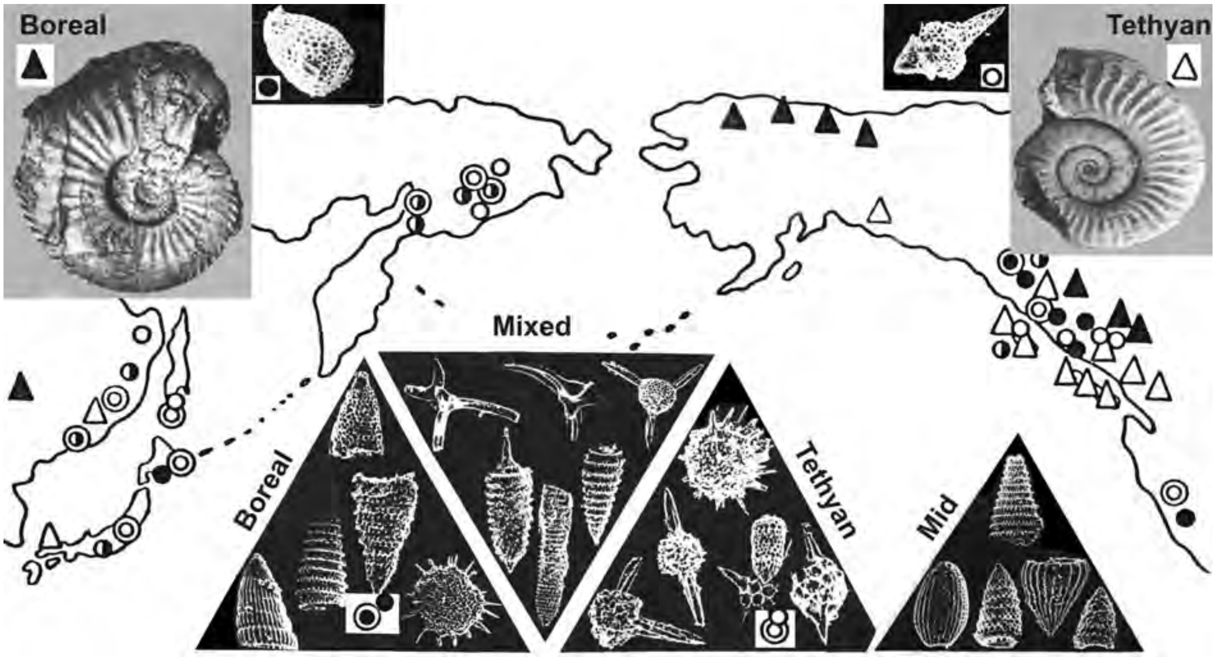


**Figure 10.** Data on biota (radiolarians and ammonites) and model for decoding the paleotectonic structure of the North Pacific framing based on radiolarian analysis. The locations of the Early Jurassic Boreal and Tethyan ammonites and radiolarians are mapped. The triangles indicate the finds of Pliensbachian ammonites. Single circles show the places of finds of Pliensbachian radiolarians, double Toarcian ones. Shaded signs indicate boreal affiliation, half shaded to belong to the northern Tethyan region, and not shaded to the Tethyan region. Modern localities of radiolarians after (Vishnevskaya 1994, 2001; Vishnevskaya and Filatova 1994; Vishnevskaya and Murchey 2002; Bragin and Bragina 2017; Bragin 2018; Cordey 2020). Modern localities of Pliensbachian boreal and Tethyan ammonites of the Alaska and Canadian Cordilleras (after Tozer *et al*. 1991). The assumed combination of different Jurassic morphological groups of radiolarians is shown in the latitudinal profile, after Filatova and Vishnevskaya (1997) .

assemblages of high paleo-latitude (southern boreal) and subequatorial types in different tectonic slices (Figure 10) (Vishnevskaya and Filatova 2016).

Depositional environments of Jurassic-Lower Cretaceous siliceous rocks and black shales are characterized on the basis of comparative facies analysis of restored stratigraphic successions (Figure 4) exposed in tectonic slices of the Koryak-Western Kamchatka orogenic belt over a distance of more than 1000 km (Figure 1). The data from this study indicate that some open oceanic areas in the mid-Mesozoic Pacific likely accommodated monotonous deposition of radiolarian-rich siliceous sediments, devoid of continental influx, while in other areas in the proximity of island arcs and in back-arc basins siliceous and tuffaceous-rich sedimentation occurred at the same time (Filatova and Vishnevskaya 1994; Cordey 1998; Orchard *et al*. 2001; Khanchuk *et al*. 2006, 2006; Al-Suwaidi *et al*. 2016; Filatova 2018).

Jurassic-Lower Cretaceous pelagic radiolarian-rich siliceous rocks in the study area form a condensed sedimentary succession of about 150 m or less of restored cumulative thickness. A common feature of the studied sections is a progressive upward change in composition (Figure 4). Hettangian red jaspers with rare layers of black shales are replaced upward by Sinemurian-Toarcian black and dark-coloured organic-rich thinly laminated cherts, siliceous shales, and siltstone. Middle Jurassic units consist of haematitic red jaspers with rare beds of black cherts that indicate gradual transition upward from Lower Jurassic black shale units. Upper Jurassic-Lower Cretaceous (Oxford ian-Barremian) units are predominantly composed of red thinly and rhythmically laminated jaspers and shales. Valan ginian-Hauterivian jaspers include limestones and rare beds of organic-rich cherts. Jurassic-Lower Cretaceous siliceous rocks do not contain any continental terrigenous clastic or pyroclastic material and were likely deposited in deep-water pelagic open-ocean environments, away from continental margins and island arcs (Figure 11). The suggested deep-water open pelagic setting is in agreement with the strong negative Ce anomaly typical for the silica-rich radiolarites of the Taigonos Peninsula that inherited REE distribution from deep ocean water (Figure 7b). Rare sandstone beds in Lower Jurassic units (Figure 4) are volcaniclastic in composition and might have been formed by turbidite or bottom currents from local topographic highs by analogy to clastic rocks in the Jurassic deposits from Sites 800 and 801 (Ogg *et al*. 1992a).

The Middle Jurassic-Lower Cretaceous (Bathonian-Valanginian) red clayey radiolarites, radiolarian-poor mudstones and Fe- and Mn-rich metalliferous radiolari

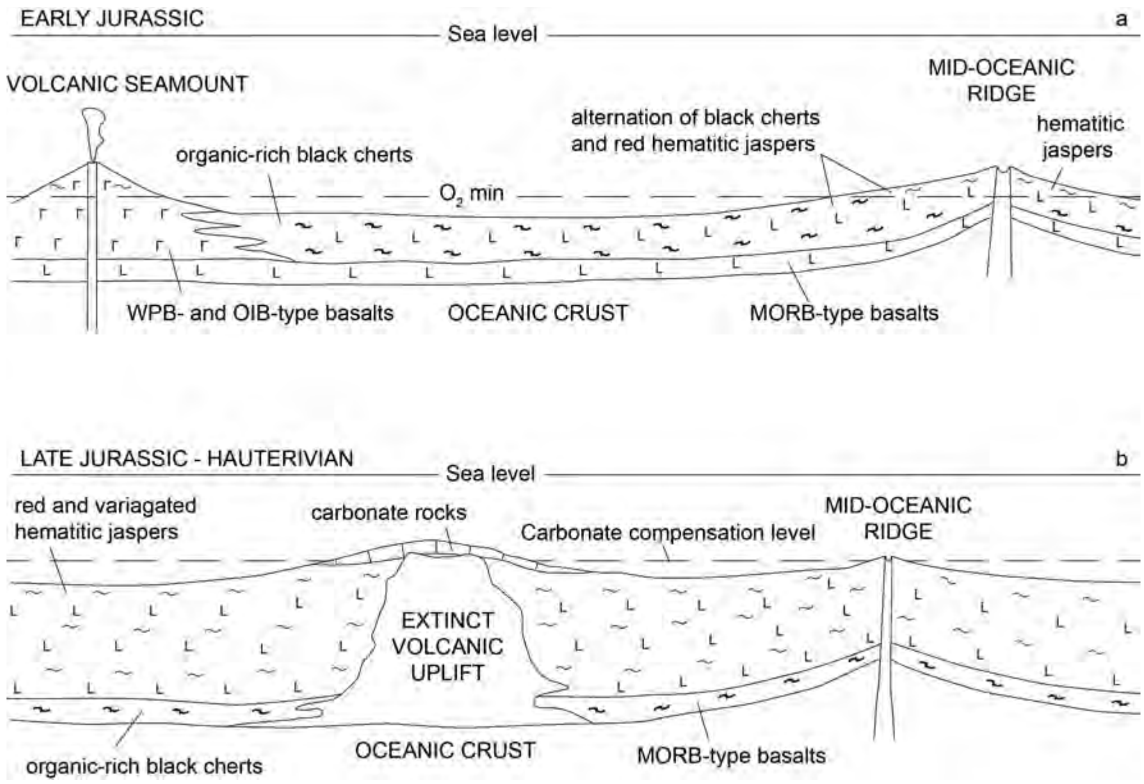


**Figure 11.** Depositional environments of siliceous rock and black shale accumulations in the Early Jurassic (a) and Late Jurassic – Hauterivian (b). $O_2$ min, oxygen minimum zone.

tes from Sites 800 and 801 in the Pacific Pigafetta Basin (Figure 9) were accumulated under oxygenated bottom water conditions at near-spreading ridge setting, similar to the present East Pacific Rise (Ogg *et al*. 1992a). The rhythmic alternation of radiolarite and claystones can be attributed to several factors, e.g. differential silica dissolution, and precipitation between the clay-rich and silica-rich layers, redeposition pulses of radiolarian-rich sediment as turbidites from adjacent margins or local topographic highs, or to distal turbidity currents. The Fe enrichment in the Jurassic-Lower Cretaceous clayey radiolarites from Sites 800 and 801 is attributed to high authigenic Fe-rich montmorillonite and other Fe-smectites in these rocks (Ogg *et al*. 1992a). Similar depositional settings close to spreading centres can be inferred for the Jurassic-Lower Cretaceous Fe- and Mn-rich rocks associated with basalt pillows (Figure 7) in the Taigonos Peninsula and Sikhote-Alin area. The accumulation of radiolarian jaspers with manganese nodules may indicate settings with seafloor surface located higher than the oxygen minimum zone because manganese is soluble in low-oxygen seawater (Hein *et al*. 1997). The overall lower (Fe+Mn)/Ti ratio and higher silica content in Triassic and Jurassic-Lower Cretaceous siliceous rocks of these regions compared to Bathonian-Valanginian clayey radiolarites of Sites 800 and 801 (Figure 7) may indicate lower content of Fe-rich clays in these rocks.

The upward replacement of red jaspers by black shales in the Early Jurassic may reflect a progressive variation through time of bottom water oxygen saturation. In the Early Hettangian, accumulation of haematitic jaspers occur red in basins with water column enriched by oxygen. In the Late Hettangian, progressively increasing deposition of dark-coloured organic-rich cherts resulted from the beginning of stagnation and deterioration of water circulation. By the end of the Hettangian, settings with poor circulation were replaced by those with euxinic conditions in which the organic-rich and pyrite-bearing thinly laminated cherts and siliceous siltstones of the black shale formation were deposited during Sinemurian-Toarcian interval (Figure 11). The transition in and out the Sinemurian-Toarcian anoxic regime in the study region was gradual with accumulation of alternating beds of dark cherts and variegated jaspers, that could reflect water fluctuations from stagnant (reduc ed Fe) to aerated (oxidized Fe) settings. The composition of siliceous deposits was likely affected by paleo-topography of the ocean and vertical zonation of aerated and anoxic depositional environments. Close to the uplifts on the ocean floor, an aquatic regime existed in the Sinemurian–Toarcian that experienced a non-equilibrium variable mode of moderate aeration and stagnation of water conditions probably caused by oxygen level fluctuations that resulted in accumulation of black organic-rich shales with lenses of haematitic jaspers (Figure 11). The elevated zones of mid-oceanic ridges and within-plate uplifts crossed the boundary of oxygen depletion of aquatic environments. Above this boundary, the zones were characterized by accumulation of lava flows and haematitic jaspers, most likely in aerated conditions above euxinic waters. Below the boundary, in the deeper setting, lenses of dark coloured cherts formed in the interstitial space between pillow-lavas.

Sinemurian-Toarcian depositional environments in the deep-sea paleo-basins were characterized by anoxic regimes that corresponded in time to within-plate magmatic activity that occurred in the Paleo-Pacific (Pankhurst *et al*. 1998; Palfy and Smith 2000; Filatova and Khain 2009) with various degrees of intensity (Ruhl *et al*. 2016; Storm *et al*. 2020).

The radiolaria-bearing black chert and shale succession of the Koryak-Western Kamchatka orogenic belt was formed during the Sinemurian-Toarcian, an interval that is longer than the generally accepted time interval for the Toarcian OAE (Jenkyns 1988, 2010). The accumulation of the studied Toarcian black shale succession corresponds in time to the global Toarcian oceanic anoxic event, while deposition of the Sinemurian-Pliensbachian black shale succession was likely controlled by regional factors. The effect of local volcanic activity could affect marine biochemistry even though such a relationship is not fully understood yet. It was shown that volcanism can favour bioavailability of key nutrients (Jones and Gislason 2008) and support phytoplankton blooms (Frogner *et al*. 2001); but it can also have negative impacts on phytoplankton communities by leaching toxic metals from ash deposited in seawater (Jones and Gislason 2008) and cause mass mortality in pteropods (Wall-Palmer *et al*. 2011). The lowest diversity of anammox bacteria was observed in deep sea sediments with the highest ash deposit near the volcanically active island of Montserrat, Lesser Antilles (Song *et al*. 2014).

Jurassic-Lower Cretaceous radiolarian-rich siliceous rocks that form layered packages, lenses and fill inter-pillow spaces within basalt lava flows of MORB-, and OIB-types (Figure 4) likely originated in settings similar to present-day mid-oceanic ridges, within-plate uplifts or oceanic islands (Figure 11). Hydrothermal volcanic siliceous solutions that were concentrated in the bottom waters around volcanic centres likely contributed to the deposition of siliceous sediments.

In the Middle Jurassic, radiolarian-bearing siliceous rocks of the Koryak-Western Kamchatka orogenic belt accumulated under settings of aerated, well-mixed waters enriched by oxygen that expanded in pelagic abyssal basins of the open Pacific, replacing the fading anoxic event (Figure 11). Thick (20–30 m) units of haematitic jaspers and argillaceous cherts started to accumulate in the Aalenian, becoming predominant with time. Only local areas of stagnant bottom waters were preserved as reflected by deposition of black shale units alternating laterally and vertically with haematitic jaspers. Jurassic cherts and jaspers contain radiolarian assemblages typical of abyssal and open-pelagic conditions reflected in their highly diverse taxonomic composition, complex shell sculpture, and the simultaneous occurrence of mature and juvenile forms (Vishnevskaya and Filatova 2017).

In the Late Jurassic–Early Cretaceous, most of the bottom waters in abyssal basins were likely well aerated and enriched in oxygen (Figure 11). At the boundary of the Middle and Late Jurassic, even local accumulation of organic-rich black shale deposits ceased, and radiolarian-bearing haematitic jaspers predominate from the Kimmeridgian to Barremian. By the end of the Late Jurassic and in the Early Cretaceous, carbonate sedimentation appeared in the form of local ammonite- and *Buchia*-bearing, *Inoceramus*-bearing limestone layers alternating with radiolarian-bearing haematitic jaspers, probably deposited in neritic marine conditions at the tops of submarine uplifts, e.g. extinct volcanos (Figure 11). Radiolarian assemblages also show signs of neritic depositional settings: relative generic uniformity, sharp dominance of mature forms and the most durable skeletons (Vishnevskaya and Filatova 2017). Oxfordian-Barremian jaspers form lenses and discontinuous layers in basalt pillow-lavas that accumulated synchronously with formation of MORB- and OIB-type basalts in intra-oceanic volcanic settings.

During the Early Cretaceous, local small basins with poorly circulated bottom waters likely existed within a general background of well-aerated waters, reflecting discontinuous distribution of a Late Valanginian and Late Hauterivian anoxic regime in different sedimentary basins (Cecca *et al*. 1993; Baudin 2005; Jenkyns 2010; Westermann *et al*. 2010). Even though these deposits had a widespread distribution, their origin is not considered to be linked to global OAEs (Westermann *et al*. 2010).

## Discussion

Jurassic – Cretaceous (Barremian) siliceous successions including organic-rich black cherts and shales (Figure 9) are recognized in other fold-and-thrust belts on the western and eastern margins of the Pacific Ocean (Robinson *et al*. 2017): Sikhote-Alin (Kemkin and Filippov 2011), Japan (Matsuoka 1995; Matsuoka *et al*. 1996; Grocke *et al*. 2011), British Columbia (Cordey and Carter 1996; Orchard *et al*. 2001; Struik *et al*. 2001), Costa Rica (Gursky and Schmidt-Effing 1982), and New Zealand (Matsuoka *et al*. 1996). Pelagic settings of the paleo-ocean were reconstructed (Grocke *et al*. 2011) for depositional environments of Early Jurassic organic-rich cherts of Japan (Figure 8). Jurassic Radiolarian assemblages of the Paleo-Pacific underwent restructuring that started in the Hettangian (Carter and Hori 2005) and reached a peak (Figure 8(c)) in the Early Toarcian (Hori 1997). Oxfordian-Berriasian siliceous rocks of Sikhote-Alin accumulated in an abyssal distal oceanic environment (Kemkin and Kemkina 2015). These deposits are thin and accumulated slowly (about 1.5 mm per 1000 years). Nearly complete suppression of carbonate sedimentation in the Pacific during the Jurassic resulted in the absence of calcareous fossils and the predominant development of Radiolarians. Benthic fauna was likely absent because no bioturbation was recognized in the Lower Jurassic siliceous deposits of the study area. Depositional environments of the Lower Jurassic Pacific black shale succession differ from settings of epi-continental basins of the Tethys (in Europe and Mediterranean area) that were characterized by accumulation of black shale associations of terrigenous and carbonate rocks (Jenkyns 1988, 2010).

The planet-wide occurrence of the Early Jurassic T-OAE was synchronous with a phase of global WPB-magmatic activity and large igneous provinces (LIPs) or silicic LIPs (SLIPs), e.g. 120 Ma Whitsunday of Australia and the c. 180 Ma Chon Aike of southern South America (Pankhurst *et al*. 1998; Palfy and Smith 2000; Prokoph *et al*. 2013; Al-Suwaidi *et al*. 2016; Xu *et al*. 2017). Plume magmatic events of LIPs in the Early Jurassic could have contributed to oxygen-depleted seawater settings by emissions of huge amounts of $CO_2$ and $SO_2$ during hydrothermal activity (Figure 12), resulting in global perturbations of carbon isotopes and accumulation of black shale formations (Jenkyns *et al*. 2001; Bailey *et al*. 2003; Svensen *et al*. 2004; Hesselbo *et al*. 2007; Gomez *et al*. 2008; Jenkyns 2010; Metodiev *et al*. 2012). Erosion of surrounding land areas contributed to water stagnation in epi-continental basins (Gavrilov 1989; Jenkyns *et al*. 2001, 2002; Metodiev *et al*. 2012; Xu *et al*. 2018). Volcanic activity that occurred in open parts of the Paleo-Pacific likely contributed to the development of euxinic water settings and sedimentation of black cherts and shales in these areas (Figure 12).

Enrichment of black shales in total organic carbon (TOC) and a negative carbon-isotope excursion (CIE) are indicators of global Early Toarcian anoxia (T-OAE). Data from black shale formations of Japan (Figure 8(c)), England and British Columbia indicate that several negative pulses carbon isotopes occurred during and preceding the T-OAE interval, indicating that in these areas, anoxia occurred in several stages (Caruthers *et al*. 2011), an inference that is supported by temperature and climatic data (Gomez *et al*. 2008; Ruhl *et al*. 2016; Arabas *et al*. 2017; Bougeault *et al*. 2017). Four large-amplitude negative shifts of $\delta^{13}C$ are recorded in Early Jurassic calcareous siltstones of the Cardigan Basin (UK): in the lowermost Hettangian, Sinemurian-Pliensbachian transition, uppermost Pliensbachian and the most important culminating CIE in the Early Toarcian (Storm *et al*. 2020). Increased TOC and higher activity of WPB-type magmatic events correspond in time to the CIEs (Ruhl *et al*. 2016; Storm *et al*. 2020). It was interpreted

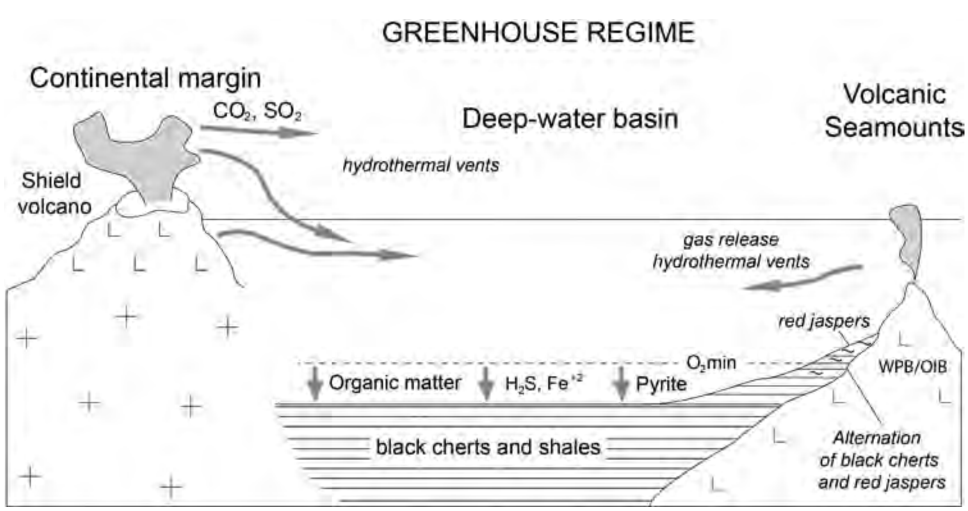


**Figure 12.** Model of climatic and depositional environments during the Early Jurassic OAE in the Paleo Pacific and corresponding geochemical parameters characterizing the accumulation of siliceous black shales.

that the Early Toarcian OAE is a global event, whereas other occurrences of black shale sedimentation likely resulted from regional conditions (Caruthers *et al*. 2011).

Accumulation of the Sinemurian – Toarcian black shale succession of the Koryak – Western Kamchatka orogenic belt can likely be correlated with variation in intensity and distribution of Early Jurassic magmatic events. Regional-scale Sinemurian – Pliensbachian magmatic activity in the Paleo-Pacific resulted in redox conditions in the oceanic water column that produced local black shale accumulation. Toarcian organic-rich cherts of the study area correspond in time with the interval of black shale accumulation during the global T-OAE and intense WPB-activity.

## Conclusions

Detailed dating of radiolarian assemblages and careful lithological correlation of allochthonous Jurassic-Lower Cre taceous siliceous rocks and black shales of the Koryak-Western Kamchatka orogenic belt helped characterize stratigraphic intervals from the Early Jurassic (Hettangian) to the Early Cretaceous (Barremian). Continuous stratigraphic siliceous successions of this time interval are reconstructed from imbricated tectonic structures of allochthonous complexes and correlated across the region over a distance of more than 1000 km.

Two main stratigraphic successions of Jurassic-Lower Cretaceous siliceous rocks and black shales are reconstructed in allochthonous lithotectonic complexes forming the imbricated tectonic structures of the Koryak-Western Kamchatka orogenic belt. The first association is represented by Hettangian and Aalenian-Barremian haematitic jaspers. The second, Sinemurian-Toarcian ass ociation includes pyrite-bearing organic-rich black cher ts and siliceous shales. Jurassic-Barremian jaspers and ch erts are also associated with basalts of MORB- and WPB-types.

The Jurassic-Barremian siliceous rocks are characterized by low restored cumulative thickness (less than 150 m), low rates of sedimentation and progressive upward chan ge in composition. Hettangian haematitic jaspers with thin layers of organic-rich rocks in the upper part are repla ced by Sinemurian–Toarcian organic-rich black shales and cherts. Middle Jurassic haematitic jaspers with rare thin layers of organic-rich rocks are overlain by Upper Jurassic–Lower Cretaceous (Berriasian–Barremian) red and variegated jaspers with rare thin layers of organic-rich black shales and ammonite and *Buchia*-bearing limestone in the Valanginian-Hauterivian interval.

Allochthonous Jurassic-Barremian siliceous successions of the Koryak-Western Kamchatka orogenic belt likely accumulated in pelagic domains of the Paleo-Pacific within the Izanagi-Kula plate at paleo-latitudes ranging from high (southern boreal) to subequatorial (northern Tethys). Hettangian and Middle Jurassic to Upper Jurassic – Barremian haematitic jaspers accumulated under aerobic water conditions with good circulation. Depositional environments of Sinemurian-Toarci an organic-rich black cherts and shales were likely euxinic deep-water paleo-oceanic settings with poor water circulation that were associated with magmatic events of the WPB-type. Similar pelagic settings of the open paleo-ocean have been reconstructed for Jurass ic-Lower Cretaceous organic-rich cherts of Japan and Sikhote-Alin. Accumulation of the Toarcian black shale succession in some pelagic domains of the Paleo-Paci fic corresponds in time to the global Toarcian oceanic anoxic event, while deposition of regionally occurring Sinemurian-Pliensbachian black shales was likely controlled by local magmatic events.

Further comparative analysis of Jurassic-Lower Cretac eous siliceous rocks and black shales from the Koryak-Kamchatka orogenic belt and other fold-and-thrust belts of the western and eastern Pacific continental margins will contribute to better understanding of variations in composition, distribution and palaeogeographic settings of these rock associations that originated in the Paleo-Pacific Ocean.

## Acknowledgments

This study was performed at the Geological Institute, Russian Academy of Sciences and supported by State Assignment of the Geological Institute Russian Academy of Sciences, state registration numbers 0135-2020-0057 and 0135-2018-003. Authors are very thankful to the Editor-in-Chief of the International Geology Review Dr. R.J. Stern and reviewers Dr. Julie Dumoulin and Professor Hugh Jenkyns for very helpful comments and suggestions that contributed to significantly improving the initial version of the manuscript, and to I.V. Beberina for help with graphic work. We thank John Wiley and Sons, Inc. and Dr. D. Grocke for granting permission for figure 8 reproduction.

## Funding

This work was supported by the State Assignment of the Geological Institute Russian Academy of Sciences, state registration numbers 0135-2020-0057 and 0135-2018-0034.

## ORCID

Elena Konstantinovskaya http://orcid.org/0000-0003-4347-4030

Valentina Vishnevskaya http://orcid.org/0000-0001-9767-1094

## References

Al-Suwaidi, A.H., Hesselbo, S.P., Damborenea, S.E., Mancenido, M.O., Jenkyns, H.C., Riccardi, A.C., Angellosi, G. N., and Baudin, F., 2016, The Toarcian Oceanic Anoxic Event (Early Jurassic) in the Neuquen Basin, Argentina: A reassessment of age and carbon isotope stratigraphy: The Journal of Geology, v. 124, p. 1–23. doi:10.1086/684831.

Ando, A., Kodama, K., and Kojima, S., 2001, Low-latitude and Southern Hemisphere origin of Anisian (Triassic) bedded chert in Inuyama area, Mino terrane, central Japan: J: Journal of Geophysical Research: Solid Earth, v. 106, p. 1973–1986. doi:10.1029/2000JB900305.

Arabas, A., Schlog, J., and Meister, C.H., 2017, Early Jurassic carbon and oxygen isotope records and belemnite rostra (Pieniny Klippen Belt, Carpathians): Palaeogeography, Pala eoclimatology, Palaeoecology. doi:10.1016/j.palaeo.2017.06.007.

Bailey, T.R., Rosenthal, J.M., McArthur, B., van de Schootbrugge, B., and Thirwall, M.C., 2003, Paleoceanographic changes of the Late Pliensbachian-Early Toarcian interval: A possible link to the genesis of on Oceanic Anoxic Event: Earth and Planetary Science Letters, v. 212, p. 307–320. doi:10.1016/S0012-821X(03)00278-4.

Basov, I.A., and Vishnevskaya, V.S., 1991, Stratigraphy of Upper Mesozoic of the sedimentary capsule of Pacific Ocean: Moscow, Nauka, p. 200.

Bau, M., Koschinsky, A., Dulsky, P., and Hein, J.R., 1996, Comparison of the partitioning behaviors of Yttrium, rare earth elements, and Titanium between hydrogenic marine ferromanganese crusts and seawater: Geochimica et Cosmochimica Acta, v. 60, p. 1709–1725. doi:10.1016/0016-7037(96)00063-4.

Baudin, F.A., 2005, Late Hauterivian short-lived anoxic event in the Mediterranean Tethys: The Faraoni event: Geosci, v. 337, p. 1532–1540. doi:10.1016/j.crte.2005.08.012.

Berezner, O.S., Stavsky, A.P., and Zlobin, S.K., 1990, Early Mesozoic vulcano-plutonic association in the north of Koryak Mountains: Izv. Acad. Nauk SSSR, Ser. Geol, no. 3, p. 31–42. [in Russian].

Bogdanov, N.A., Solovyov, A.V., and Ledneva, G.V., 2003, Structure of a Cretaceous accretionary prism Omgon ridge: Geotectonics, v. 37, no. 4, p. 64–76. [in Russian].

Bond, D.P.G., and Wignall, P.B., 2014, Large igneous provinces and mass extinctions: Volcanism, impacts, and mass extinctions: causes and effects, v. 505, p. 25–35.

Bondarenko, G.E., Sokolov, S.D., and Morozov, O.L., 2008, Paleotectonic setting of Mesozoic volcanism of the southern part of the Taigonos peninsula (northeast Priokhotye): Bull. Mosk. Ob-va Ispyt. Prirody, v. 83, no. 1, p. 9–28. [in Russian].

Bougeault, C., Pellenard, P., Deconinc, J.-F., Hesselbo, S.P., Dommergues, J.-L., Brneau, L., Cocquerez, T.H., Lafont, R., Huret, E., and Thibault, N., 2017, Climatic and paleoceanographic changes during the Pliensbachian (Early Jurassic inferred from clay mineralogy and stable isotope (C-O) geochemistry (NW Europe): Global and Planetary Change, v. 149, p. 139–152. doi:10.1016/j.gloplacha.2017.01.005.

Bragin, N.Y., 2018, Jurassic and Early Cretaceous radiolarians of siliceous sequences of the Vaamychgyn–Podgornaya Interfluve, Econai Zone, Koryak Highland: Stratigraphy and Geological Correlation, v. 26, no. 3, p. 333–343. doi:10.1134/S0869593818030036.

Bragin, N.Y.U., and Bragina, L.G., 2017, Early and Middle Jurassic (Pliensbachian to Bajocian) Radiolaria from cherts of Kiselevka–Manoma accretionary complex (Amur River, eastern Russia): Ofiloiti, v. 42, no. 1, p. 3–19.

Carter, E., Whalen, P., and Guex, J., 1998, Biochronology and paleontology of Lower Jurassic (Hettangian and Sinemurian) radiolarians, Queen Charlotte Islands, British Colombia: Geologica Survey of Canada Bulletin, v. 496, p. 162.

Carter, E.S., and Hori, R., 2005, Global correlation of the radiolarian faunal change across the Triassic-Jurassic boundary:: Canadian Journal of Earth Sciences, v. 42, p. 777–790. doi:10.1139/e05-020.

Caruthers, A.H., Grocke, D.R., and Smith, P.L., 2011, The significance of an Early Jurassic (Toarcian) carbon-isotope excursion in Haida Gwaii (Queen Charlotte Islands), British Columbia, Canada: Earth and Planetary Science Letters, v. 307, p. 19–26. doi:10.1016/j.epsl.2011.04.013.

Cecca, F., Marini, A., Pallini, G., Baudin, F., and Begouen, V., 1993, A guide-level of the uppermost Hauterivian (Lower Cretaceous) in the pelagic succession of Umbria-Marche (Central Italy): The Faraoni level: Rivista italiana di Paleontol ogia e Stratigrafia, v. 90, p. 551–568.

Chamov, N.P., and Andreev, A.V., 1997, The Middle Jurassic-Lower Cretaceous sedimentary complexes in the accretionary structure of the Peninsula Taygonos: Lithology and Mineral Resources, v. 32, no. 3, p. 260–272. [in Russian].

Cordey, F., 1998, Radiolaries des complexes d,accretion de la Cordillere Canadienne (Colombie-Britannique): Commission géologique du Canada, v. 509, p. 209.

Cordey, F., 2020, Timing of Cache Creek Ocean closure: Insights from new Jurassic radiolarian ages in British Columbia and Yukon and their significance for Canadian Cordillera tectonics: Canadian Journal of Earth Sciences, v. 57, p. 1167–1179. doi:dx.doi.org/10.1139/cjes-2019-0236.

Cordey, F., and Carter, E.S., 1996, New Nasselaria (Radiolaria) from the Lower Jurassic of the Canadian Cordillera: Canadian Journal of Earth Sciences, v. 33, p. 444–451. doi:10.1139/e96-034.

Farrimond, P., Stoddart, D.P., and Jenkyns, H.C., 1994, An organic geochemical profile of the Toarcian anoxic event in northern Italy: Chemical Geology, v. 111, p. 168–191. doi:10.1016/0009-2541(94)90080-9.

Filatova, N.I., 1998, Cretaceous evolution of continental margins in the context of other global events: Stratigraphy and Geological Correlation, v. 6, p. 1–15. [in Russian].

Filatova, N.I., 2014, New data on the tectonic position of the Mesozoic rocks of Western Kamchatka in the structures of the Middle Cretaceous orogenic belt in Eastern Asia: Doklady Earth Sciences, v. 455, p. 556–561. doi:10.1134/S1028334X1405002X.

Filatova, N.I., 2018, Extent of the Middle Cretaceous Orogenic Belt in Eastern Asia and the geodynamic causes of its transformation: Doklady Earth Sciences, v. 478, p. 194–198. doi:10.1134/S1028334X18020228.

Filatova, N.I., Dvoryankin, A.I., and Milekhin, A.I., 1990, Jurassic-Neocomian formations and tectonics of the Western Rarytkyn zone of the Koryakiya: Izvestia Vuzov, Ser. Geol., no. 12, p. 3–17. [in Russian].

Filatova, N.I., and Khain, V.E., 2009, Structure of the Central Arctic and their relation to the Mesozoic Arctic plume: Geotectonics, v. 43, p. 462–489. doi:10.1134/S0016852109060028.

Filatova, N.I., and Vishnevskaya, V.S., 1994, Tectonic position of the Mesozoic ophiolitic and island arc formations in the Koryak Region (Northeastern Russia), *in* Proceedings, 29th International Geol. Congress, Ophiolite Symposium, Netherl ands, P.D. VSP, p. 109–127.

Filatova, N.I., and Vishnevskaya, V.S., 1997, Radiolarian stratigraphy and origin of the Mesozoic terranes from the continental framework of the northwestern Pacific (Russia): Tectonophysics, v. 269, p. 131–150. doi:10.1016/S0040-1951(96)00156-4.

Frogner, P., Gislason, S.R., and Oskarsson, N., 2001, Fertilizing potential of volcanic ash in ocean surface water: Geology, v. 29, p. 487–490. doi:10.1130/0091-7613(2001)029<0487:FPOVAI>2.0.CO;2.

Gavrilov, Y.O., 1989, , Sedimentation in an Early Jurassic of a Large Caucasus (links to transgressions and regressions): Lithology and Mineral Resources, no. 2, p. 3–15. [in Russian].

Gavrilov, Y.O., Shepetova, E.V., Baraboshkin, E.Y., and Shcherbinina, E.A., 2002, Early Cretaceous anoxic basins of the Russian plate: Sedimentology and geochemistry: Lithology and Mineral Resources, v. 37, no. 4, p. 359–380. [in Russian].

Gomez, J.J., Goy, A., and Canales, M.L., 2008, Seawater temperature and carbon-isotope variations in belemnites linked to mass extinction during the Toarcian (Early Jurassic) in Central and Northern Spain. Comparison with other European sections: Palaeogeography, Palaeoclimatology, Palaeoecology, v. 258, p. 28–58. doi:10.1016/j.palaeo.2007.11.005.

Grigor'ev, V.N., Sokolov, S.D., Krylov, K.A., Golozubov, V.V., and Pral'nikova, I.E., 1995, Geodynamic typification of the Triassic–Jurassic Effusive Siliceous complexes of the Kuyul Terrane (Koryak Highland): Geotektonika, v. 30, no. 3, p. 59–69. [in Russian].

Grocke, D., Hori, R., Trabucho-Alexandre, J., Kemp, D., and Schwark, L., 2011, An open ocean record of the Toarcian oceanic anoxic event: Solid Earth, no. 3, p. 245–257. doi:10.5194/se-2-245-2011.

Gursky, H.J., and Schmidt-Effing, R., 1982, Chapter 9 Sedimentology of Radiolarites Within the Nicoya Ophiolite Complex, Costa Rica, Central America Developments in Sediment v. 36, p. 127–145.

Hein, J.R., Koschinsky, A., Halbach, P., Manheim, F.T., Bau, M., Kang, J.-K., and Lubick, N., 1997, Iron and Manganese Oxide Mineralization in the Pacific, Manganese Mineralization: Geochemistry and Mineralogy of Terrestrial and Marine Deposits: Geol. Soc. Special Publ., Vol. 119, p. 123–138. London, Geological Society of London.

Hein, J.R., Yeh, H.-W., Gunn, S.H., Sliter, W.V., Benninger, L.M., and Wang, C.-H., 1993, Two major Cenozoic episodes of phosphogenesis recorded in equatorial Pacific seamount deposits: Paleoceanography, v. 8, p. 293–311. doi:10.1029/93PA00320.

Hesselbo, S.P., Jenkyns, H.C., Duarte, L.V., and Oliveria, L.C., 2007, Carbon-isotope record of the Early Jurassic (Toarcian) Oceanic Anoxic Event from fossil wood and marine carbonate (Lusitanian Basin, Portugal): Earth and Planetary Science Letters, v. 253, p. 455–470. doi:10.1016/j.epsl.2006.11.009.

Hori, R., 1992, Radiolarian biostratigraphy in the Triassic-Jurassic Period boundary in bedded cherts from the Inuyama area, central Japan: J. Geosci. Osaca City Univ., v. 35, p. 53–65.

Hori, R., 1997, The Toarcian radiolarian event in bedded cherts from southwestern Japan: Marine Micropaleontology, v. 30, p. 159–169. doi:10.1016/S0377-8398(96)00024-2.

Hori, R., Fudjiki, T., Inoue, E., and Kimura, J.-I., 2007, Platinum group element anomalies and bioevents in the Triassic-Jurassic deep-sea sediments of Panthalassa: Palaeogeography, Palaeoc limatology, Palaeoecology, v. 244, p. 391–406.

Ikeda, M., Hori, R.S., Ikehara, M., Miyashita, R., Chino, M., and Yamada, K., 2018, Carbon cycle dynamics linked with Karoo-Fer rar volcanism and astronomical cycles during Pliensbachian-Toarcian (Early Jurassic): Global and Planetary Change, v. 170, p. 163–171. doi:10.1016/j.gloplacha.2018.08.012.

Jenkyns, H.C., 1988, The early Toarcian (Jurassic) anoxic event: Stratigraphic, sedimentary, and geochemical evidence: American Journal of Science, v. 288, p. 101–151.

Jenkyns, H.C., 2010, Geochemistry of oceanic anoxic events: Geochemistry, Geophysics, Geosystems, v. 11, p. 1–18.

Jenkyns, H.C., Croke, D.L., and Hesselbo, S.P., 2001, Nitrogen isotope evidence for water mass denitrification during Early Toarcian (Jurassic) oceanic anoxic event: Paleooceanology, v. 16, p. 593–603.

Jenkyns, H.C., Jones, C.E., Crocke, D.E., Hesselbo, S.P., and Parkinson, D.N., 2002, Chemostratigraphy of the Jurassic System: Applications, limitations, and implications for palaeoceanography: Journal of the Geological Society, v. 159, p. 351–378. doi:10.1144/0016-764901-130.

Jenkyns, H.C., and Winterer, E.L., 1982, Palaeoceanography of Mesozoic ribbon radiolarites: Earth and Planetary Science Letters, v. 60, p. 351–375. doi:10.1016/0012-821X(82)90073-5.

Jones, M.T., and Gislason, S.R., 2008, Rapid releases of metal salts and nutrients following the deposition of volcanic ash into aqueous environments: Geochimica et Cosmochimica Acta, v. 72, p. 3661–3680. doi:10.1016/j.gca.2008.05.030.

Kemkin, I.V., and Filippov, A., 2011, New finds of Middle and Late Jurassic Radiolarians in the Siliceous-Clayey and Clastic Rocks of the Nadankhada-Bikin Terrane (Jurassic Accretionary Wedge, Western Sikhote-Alin) and Their Geological Significance: Russian Journal of Pacific Geology, p. 518–530. doi:10.1134/S1819714011060066.

Kemkin, I.V., and Kemkina, R.A., 2004, Structure and age of the siliceous-terrigenous sediments of the lower structural units Taukhin terrane (South Sikhote-Alin): Russian Journal of Pacific Geology, v. 23, no. 5, p. 68–80. [in Russian].

Kemkin, I.V., and Kemkina, R.A., 2015, Geochemical evidences for the oceanic origin of cherts of the accretionary complexes of the Sikhote-Alin: Russian Journal of Pacific Geology, v. 60, no. 8, p. 706–719. [in Russian].

Kemkin, I.V., Palandzhyan, S.A., and Chekhov, A.D., 1996, Evidences of the age of siliceous-volcanogenic complexes of the Povorotny Cape, Penzhinsko-Pekulneysky ophiolite belt: Russian Journal of Pacific Geology, v. 15, p. 69–78. [in Russian].

Kemp, D.B., and Izumi, K., 2014, Multiproxy geochemical analysis of a PanThalassaic margin record of the early Toarcian oceanic anoxic event (Toyora area, Japan): Palaeogeography, Palaeoclimatology, Palaeoecology, v. 415, p. 332–341. doi:10.1016/j.palaeo.2014.09.019.

Khanchuk, A.I., Golozubov, V.V., Goryachev, N.I., and Rodionov, S. M., 2006, Geodynamic reconstructions and metallogeny of East of Russia, *in* Khanchuk, A.I., ed., Geodynamics, magmatism and metallogeny of Russia, Dalnauka: Vladivostok, book 2, p. 880–897. [in Russian].

Khanchuk, A.I., Golozubov, V.V., and Panchenko, I.V., 1992, Ganychalansky terrane of the Koryak uplands: Russian

Journal of Pacific Geology, v. 2, no. 4, p. 82–93. [in Russian].

Khanchuk, A.I., Grigoriev, V.N., and Golozubov, V.V., 1990, Kuylski ophiolite terrane: Vladivostok, Far-Eastern Branch USSR Acad. Sci., p. 108 p. [in Russian].

Kholodov, V.N., 2002, On the role of hydrogen sulfide basins in sedimentary ore formation: Lithology and Mineral Resources, v. 37, no. 5, p. 451–473. [in Russian].

Klinkhammer, G., Elderfield, H., and Hudson, A., 1983, Rare earth elements in seawater near hydrothermal vents: Nature, v. 305, p. 185–188. doi:10.1038/305185a0.

Konstantinovskaya, E.A., 1998, Mesozoic oceanic siliceous, carbonate, and terrigenous rocks at the southeastern Taigonos Peninsula (Northeastern Russia): Lithology and Mineral Resources, v. 33, no. 4, p. 354–368.

Krymsalova, V.T., 1994, Radiolaria and stratigraphy of the volcanogenic-siliceous deposits of Mesopotamia, Talain-Pravyi Trainyn: Russian Journal of Pacific Geology, no. 1, p. 121–124. [in Russian].

Marshall, M., 2013, Biostratigraphy and lithostratigraphy of the Middle Jurassic Tecocoyunga Group, Mexico: Comptes Rendus Geoscience, v. 345. doi:101016/j.crte.2013.03.00,1-283.

Matsuoka, A., 1992, Jurassic and Early Cretaceous radiolarians from Leg 129, Sites 800 and 801, Western Pacific Ocean, *in* Proc. ODP, Sci. Results, v. 129, p. 203–220.

Matsuoka, A., 1995, Jurassic and Lower Cretaceous radiolarian zonation in Japan and in the western Pacific: The Island Arc, v. 4, p. 140–153. doi:10.1111/j.1440-1738.1995.tb00138.x.

Matsuoka, A., Aita, Y., Wakita, K., Shen, G., Ujiie, H., Sashida, K., Vishnevskaya, V., Bragin, N., and Cordey, F., 1996, Mesozoic radiolarians and radiolarian-bearing sequences in the circum-Pacific regions: A report of the symposium "Radiolari ans and Orogenic Belts": The Island Arc, no. 5, p. 203–213. doi:10.1111/j.1440-1738.1996.tb00026.x.

McLennan, S.M., and Taylor, S.R., 1981, Role of subducted sediments in Island-Arc Magmatism: Constraints from REE Patterns: Earth and Planetary Science Letters, v. 54, p. 423–430. doi:10.1016/0012-821X(81)90058-3.

Metodiev, L., Savov, I.P., Grocke, D., Wignall, P., Newton, R., Andreeva, P., and Koleva, E., 2012, Paleo-environmental conditions recorded by $^{87}Sr/^{86}Sr$, $\delta^{13}C$ and $\delta^{18}O$ in Late Pliensbach ian-Toarcian (Jurassic) belemnites from Bulgaria: Solid Earth Discussions, v. 4, p. 315–361. doi:10.5194/sed-4-315-2012.

Michard, A., Albarede, F., Michard, G., Minster, J.F., and Charlou, J.L., 1983, Rare-earth elements and Uranium in high-temperature solutions from East Pacific rise hydrothermal vent field (13°N): Nature, v. 303, p. 795–797. doi:10.1038/303795a0.

Muller, R., Sdrolias, M., Gaina, C., and Roest, W., 2008, Age, spreading rates, and spreading asymmetry of the worlds ocean crust: Geochemistry, Geophysics, Geosystems, v. 9, p. Q04006. doi:10.1029/2007GC001743.

Nokleberg, E.A., Parfenov, L.M., and Monger, J.W.H., 1994, Circum North Pacific tectonostratigrafic terrane map: U.S. Geol. Surv.Open File Rep., v. 7, 94–114.

Ogg, J.G., Karl, S.M., and Behl, R.J., 1992a, Jurassic through Early Cretaceous sedimentation history of the central equatorial Pacific and of Sites 800 and 801, *in* Larson, R.L., Lancelot, Y., et al., eds., Proceedings of the Ocean Drilling Program, Scientific Results, College Station, TX (Ocean Drilling Program), p. 129, 571–613. doi:10.2973/odp.proc.sr.129.117.1992.

Ogg, J.G., Karl, S.M., and Behl, R.J., 1992b, Chemistry and accumulation rates of Jurassic to early Cretaceous sediments from the central equatorial Pacific. PANGAEA. Supplement to (Ogg et al., 1992a) doi:10.1594/PANGAEA.779283

Orchard, M.J., Cordey, F., Rui, L., Bamber, E.W., Mamet, B., Struik, L. C., Sano, H., and Taylor, H.J., 2001, Biostratigraphic and biogeographic constraints on the carboniferous to Jurassic Cache Creek Terranes in central British Columbia: Canadian Journal of Earth Sciences, v. 38, p. 551–578. doi:10.1139/e00-120.

Palfy, J., and Smith, P.L., 2000, Synchrony between Early Jurassic extinction, oceanic anoxic event, and the Karoo-Ferrar Flood basalt volcanism: Geology, v. 28, p. 747–750. doi:10.1130/0091-7613(2000)28<747:SBEJEO>2.0.CO;2.

Pankhurst, R., Leat, P.H.T., Sruoga, P., and Riley, T.R., 1998, The Chon Aike province of Patagonia and related rocks in West Antarctica: A silicic large igneous province: Journal of Volcanology and Geothermal Research, v. 8, p. 113–136. doi:10.1016/S0377-0273(97)00070-X.

Pessagno, E.A., Jr, Blome, C.D., Hull, D., and Six, W.M., 1993, Jurassic radiolaria from the Josephine Ophiolites and overlying strata. Smith River Subterrane (Klamath Mounts). Southwestern California and southwestern Oregon: Micropaleontology, v. 39, p. 93–166. doi:10.2307/1485837.

Pessagno, E.A., Jr, Canta-Chapa, A., Mattinson, J.M., Meng, X., and Kariminia, S.M., 2009, The Jurassic-Cretaceous boundary: New data from North America and Caribbean: Stratigraphy, v. 6, p. 185–262.

Pessagno, E.A., Jr., and Martin, C., 2003, Tectonostratigraphic evidence for the origin of the Gulf of Mexico, *in* Bartolini, C., Buffer, R.T., and Blickwede, J., eds., The Circum-Gulf of Mexico and Caribbean: Hydrocarbon habitus, basin formation, and plate tectonics: AAPG Memoir, American Association of Petroleum Geologists, v. 79, \, p. 46–74.

Peyve, A.A., 1984, Structure and structural position of ophiolites of the Koryak Ridge: Moscow, Nauka, p. 99 p. [in Russian].

Prokoph, A., El Bilali, H., and Ernst, R., 2013, Periodicities in the emplacement of large igneous provinces through the Phanerozoic: Relations to ocean chemistry and marine biodiversity evolution: Geoscience Frontiers, v. 4, p. 263–276. doi:10.1016/j.gsf.2012.08.001.

Robinson, S.A., Heimhofer, U., Hesselbo, S., and Petrizzo, M.R., 2017, Mesozoic climates and oceans – a tribute to hugh Jenkyns and Helmut Weissert: Sedimentology, v. 64, p. 1–15. doi:10.1111/sed.12349.

Robinson, S.A., Williams, T., and Bown, P.R., 2004, Fluctuations in biosiliceous production and the generation of Early Cretaceous oceanic anoxic events in the Pacific Ocean (Shatsky Rise, Ocean Drilling Program Leg 198): Paleoceanography, v. 19, no. 4, p. PA4024. doi:10.1029/2004PA001010.

Ruhl, M., Hesselbo, S.P., Hinnov, L., Jenkyns, H.C., Xu, W., Riding, J.B., Storm, M., Minisini, D., Ullmann, C.V., and Leng, M.J., 2016, Astronomical constraints on the duration of the Early Jurassic Pliensbachian Stage and global climatic fluctuations: Earth and Planetary Science Letters, v. 1, p. 1–17.

Ruzhentsev, S.V., Byalobzhesky, S.G., and Grigoryev, V.N., 1982, Tectonics of the Koryak Ridge: Moscow, Nauka, p. 212. [in Russian].

Scotese, C.R., 1997, Paleogeographic Atlas: PALEOMAP Progress Report, Dept. Geology, University Texas, Arlington, 45.

Shibuya, H., and Sasajima, S., 1986, Paleomagnetism of red cherts: A case study in the Inuyama area central Japan: Journal of Geophysical Research, v. 91, p. 14105–14116. doi:10.1029/JB091iB14p14105.

Sokolov, S.D., Grigoriev, V.N., and Peyve, A.A., 1996, Elements of the structural and real ordering in the serpentinite melanges: Geochemics, v. 1, p. 47–62. [in Russian].

Sokolov, S.D., Luchitskaya, M.V., Silantiev, S.E., and Morozov, O.L., 2003, Ophiolites in accretionary complexes along the early Cretaceous margin of NE Asia: Age, composition, and geodynamic diversity, in Dilec, Y., and Robinson, P.T., eds., Ophiolites in earth history: London, Spec. Publ. Geol. Society, Vol. 218, p. 619–614.

Song, B., Buckner, C.T., Hembury, D.J., Mills, R.A., and Palmer, M.R., 2014, Impact of volcanic ash on anammox communities in deep sea sediments: Environmental Microbiology Reports, v. 6, no. 2, p. 159–166. doi:10.1111/1758-2229.12137.

Storm, M.S., Hesselbo, S.P., Jenkyns, H.C., Ruhl, M., Ullmann, C. V., Xu, W., Leng, M.J., Riding, J.B., and Gorbanenko, O., 2020, Orbital pacing and secular evolution of the Early Jurassic carbon cycle: Proceedings of the National Academy of Sciences of the United States of America, v. 117, p. 3974–3982, doi: 10.1073/pnas.1912094117.

Struik, L., Schiarizza, P., Orchard, M., Cordey, F., Sano, H., Macinintyre, D., Lapierre, H., and Tardy, M., 2001, Imbricate architecture of the upper Paleozoic to Jurassic oceanic Cache Creek Terrane, central British Columbia: Canadian Journal of Earth Sciences, v. 38, p. 495–514. doi:10.1139/e00-117.

Svalnov, V.N., and Gordeev, V.V., 1986, Chemical composition of sediments, *in* Ferromanganese micronodules of the central part of the Pacific Ocean: Institute of Oceanology AN SSSR, Moscow, Russia, v. 122, p. 122. [in Russian].

Svensen, H., Planke, S., Chevallier, L., Malthe-Sorenssen, A.M., Corfu, F., and Jamtveit, B., 2004, Hydrothermal venting of greenhouse gases triggering Early Jurassic global warming: Earth and Planetary Science Letters, v. 256, p. 554–566. doi:10.1016/j.epsl.2007.02.013.

Terekhova, G.P., and Shmakin, V.B., 1982, On the geological structure of the Semiglavaya mountain: Izv. SSSR Acad. Sci., Ser. Geol., no. 4, p. 18–32. [in Russian].

Tozer, E.T., Nassichuk, W.W., Smith, P.L., and Tozer, H.W., 1991, Fossils and terranes: Evidence for dissecting the Cordillera: GEOS, v. 20, no. 3, p. 20–27.

Vishnevskaya, V.S., 1994, Early Jurassic radiolarians from the North-East of Russia: Academy of Sciences, Transactions, v. 335, no. 6, p. 757–752.

Vishnevskaya, V.S., 2001, Radiolarian biostratigraphy of the Jurassic and Cretaceous of Russia: Moscow, GEOS, p. 376.

Vishnevskaya, V.S., and Filatova, N.I., 1994, Mesozoic terranes of the northwest Pacific continental margin (Russia): Radiolarian ages and sedimentary environments: The Island Arc, v. 3, p. 199–220. doi:10.1111/j.1440-1738.1994.tb00107.x.

Vishnevskaya, V.S., and Filatova, N.I., 2008, Correlation of the Jurassic-Cretaceous siliceous-volcanogenic sediments in northwestern surroundings of the Pacific (Koryak Upland): Stratigraphy and Geological Correlation, v. 16, p. 618–638. doi:10.1134/S0869593808060038.

Vishnevskaya, V.S., and Filatova, N.I., 2012, Allochthonous Mesozoic marine sequences its of Northeast Asia and western North America: Correlation of stratigraphic levels and geodynamic depositional settings: Russian Journal of Pacific Geology, v. 6, no. 3, p. 189–208. doi:10.1134/S1819714012030074.

Vishnevskaya, V.S., and Filatova, N.I., 2016, Sedimentary settings of marine Middle Mesozoic allochthonous complexes of Northeastern Asia and their correlation: Stratigraphy and Geological Correlation, v. 24, no. 6, p. 575–592.

Vishnevskaya, V.S., and Filatova, N.I., 2017, Paleoclimatic and paleolatitude settings of accumulation of radiolarian siliceous-volcanogenic sequences in the Middle Mesozoic Pacific: Evidence from allochthons of East Asia: Oceanology, v. 57, no. 5, p. 757–773. doi:10.1134/S0001437017050186.

Vishnevskaya, V.S., and Filatova, N.I., 2018, Global climate change and the temperature regime of the Mesozoic marine environment in Northeastern Asia: Doklady Earth Sciences, v. 482, no. Part 1, p. 1147–1151. doi:10.1134/S1028334X18090209.

Vishnevskaya, V.S., and Murchey, B., 2002, Climatic affinity and possible correlation of Jurassic to Lower Cretaceous radiolarian assemblages, Russia and North America: Micropaleontology, v. 48, no. 1, p. 89–111.

Vishnevskaya, V.S., Sokolov, S.D., Bondarenko, G.E., and Pralnikova, I.E., 1998, New data on age and correlation of volcanogenic-siliceous complexes of the northwest coast of the Sea of Okhotsk: Dokl: Earth Science, v. 359, no. 1, p. 196–199.

Volokhin, Y.G., 2013, Mesozoic and Cenozoic siliceous sedimentation in Eastern Asian margin basins: Vladivostok, Dalnauka, p. 434. [in Russian].

Volokhin, Y.G., and Ivanov, V.V., 2007, Geochemistry and metal potential of Triassic carbonaceous silicites in Sikhote Alin: Lithology and Mineral Resources, v. 42, p. 363–383. doi:10.1134/S0024490207040049.

Volokhin, Y.G., Khanchuk, A.I., Ivanov, V.V., Kazachenko, V.T., and Sattarova, V.V., 2005, Geochemistry and gold content of the Triassic carbonaceous cherts of the Sikhote-Alin, Russia. *in* Mao, J., and Bierlein, F.P. (Eds), Mineral Deposits Research: Meeting the Global Challenge. Proceedings of the Eight Biennial SGA Meeting, Beijing, China, 18-21 August 2005, Volume. 1, chapter 2-29.

Wall-Palmer, D., Jones, M.T., Hart, M.B., Fisher, J.K., Smart, C.W., Hembury, D.J., et al, 2011, Explosive volcanism as a cause for mass mortality of pteropods: Marine Geology, v. 282, p. 231–239. doi:10.1016/j.margeo.2011.03.001.

Westermann, S., Folmi, K.B., Adatte, T.H., Matera, V., Schnyder, J., Fleitmann, D., Fiet, N., Ploch, I., and Duchamp-Alphonse, S., 2010, The Valanginian $\delta^{13}$C excursion may not be an expression of a global oceanic anoxic event: Earth and Planetary Science Letters, v. 290, p. 118–131. doi:10.1016/j.epsl.2009.12.011.

Wignall, P.B., Bond, D.P.G., Kuwahara, K., Kakuwa, Y., Newton, R.J., and Pulton, S.W., 2010, An 80 million-year oceanic redox history from Permian to Jurassic pelagic sediments of the Mino-Tanba terrane, SW Japan, and origin of four mass extinctions: Global and Planetary Change, v. 71, p. 109–123. doi:10.1016/j.gloplacha.2010.01.022.

Xu, W., Ruhl, M., Jenkyns, H.C., Hesselbo, S.P., Riding, J.B., Selby, D., Naafs, B.D.A., Weijers, J.W.H., Pancost, R.D., Tegelaar, E.W., and Idiz, E.F., 2017, Carbon sequestration in an expanded lake system during the Toarcian oceanic anoxic event: Nature Geoscience, v. 10, p. 129–134. doi:10.1038/ngeo2871.

Xu, W., Ruhl, M., Jenkyns, H.C., Leng, M.J., Jennifer, M.H., Minisini, D., Ullmann, C.V., Ridig, J.B., Weijers, J.W.H., Storm, M.S., Percival, L. M.E., Tosca, M.J., Idiz, E.F., Tegelaar, E.W., and Hesselbo, S.P., 2018, Evolution of the Toarcian (Early Jurassic) carbon-cycle and global climatic controls on local sedimentary processes (Cardigan Bay Basin, UK): Earth and Planetary Science Letters, v. 484, p. 396–411. doi:10.1016/j.epsl.2017.12.037.

Zlobin, S.K., Filatova, N.I., and Dvoryankin, A.I., 1992, Composition and origin of the Upper Jurassic-Lower Cretaceous volcanics of Koryak Highland: NW Pacific, Ofio liti, Vol. 1, p. 99–115.